Localization and Physiology of Zinc

In the Vertebrate Retina

Submitted by

Stephen M. Redenti

A dissertation submitted to the Graduate Faculty in Biology in partial fulfillment of the requirements for the degree of Doctor of Philosophy, The City University of New York

2006

UMI Number: 3213158

UMI Microform 3213158

ProQuest Information and Learning Company
300 North Zeeb Road
P.O. Box 1346
Ann Arbor, MI 48106-1346

This manuscript has been read and accepted for the Graduate Faculty in Biology in satisfaction of the dissertation requirement for the degree of Doctor of Philosophy.

Date	Chair of Examining Committee Dr. Richard L. Chappell, Hunter College
Date	Executive Officer Dr. Richard L. Chappell, Hunter College
	Dr. James Gordon, Hunter College
	Dr. Thomas Schmidt-Glenewinkel, Hunter College
	Dr. Pokay Ma, Queens College
	Dr. William Sieple, NYU School of Medicine

Supervision Committee

The City University of New York

Abstract

Localization and Physiology of Zn^{2+} in the Vertebrate Retina

Stephen M. Redenti

Advisor: Professor Richard L. Chappell

A growing body of evidence indicates that zinc is essential for signaling and survival of neurons in the central nervous system. In the retina endogenous zinc modulates a number of cell and receptor subtypes. The focus of this dissertation is to examine the zinc content in living retinal tissue and measure its neuromodulatory effects. Results show the presence of zinc in all retinal layers and indicate a general downmodulation of synaptic transmission at the level of the outer plexiform layer. Evidence suggests a pool of zinc associated with synaptic vesicles in photoreceptor terminals. By removing zinc released into the synapse between photoreceptors, horizontal, and bipolar cells, whole cell patched horizontal cell inward currents were significantly enhanced. With synaptic zinc removed *in situ,* increased amplitudes in the b-wave of the electroretinogram (ERG) were recorded in both pure-rod and duplex retina and shifts in sensitivity observed. Zinc concentration in synaptic vesicles is regulated by zinc transporter -3 (ZnT-3) of the SLC30 family of transporters. Retinal slices incubated with antibodies directed against the ZnT-3 protein showed localization in the regions of the inner segments, outer nuclear, and ganglion cell layers. Examination of isolated retinal cell ZnT-3 localization revealed consistent reactivity of glial

Mueller cell soma and endfeet. This finding suggests that ZnT-3 may be involved in zinc transport via Mueller cells in addition to its established role in vesicular membranes. When intracellular retinal zinc was imaged using a membrane-permeant fluorescent zinc probe, results showed high concentrations in photoreceptor outer segments with lower levels in ganglion and plexiform layers. For intracellular zinc to function as a retinal neuromodulator, synaptic release would be necessary. By depolarizing retinal slices, in the presence of a membrane-impermeant fluorescent zinc probe, release of synaptic zinc was visualized in the region of phototoreceptor outer segments and the outer plexiform layer. Over time, increased extracellular zinc was visualized spreading across all retinal layers.

Zinc homeostasis is essential to retinal function from transcription factor activation to cell surface receptor modulation. Imbalances in retinal zinc levels contribute to Age-Related Macular Degeneration, night blindness, ocular immune suppression and apoptosis. Greater understanding of retinal zinc activity will be essential for delineating mechanisms of neural processing in health and disease.

Acknowledgments

I would like to express my deepest gratitude to Dr. Richard Chappell for being a generous and supportive mentor and friend.

Thank you Joan Reid for years of valuable advice.

Hunter College Biology Department Faculty and Students

Dr. William Cohen: Dr. Joseph Lee and Alex Braun

Dr. Ben Ortiz: Dr. Faith Harrow

Dr. Patricia Rockwell: Evan Gomez, Jennifer Martinez and Luena Papa

Dissertation Committee

Dr. James Gordon

Dr. Thomas Schmidt-Glenewinkel

Dr. Pokay Ma

Dr. William Sieple

Collaborators

Dr. Christopher Frederickson: University of Texas, College of Medicine, Galveston TX.

Dr. Richard Palmiter: University of Washington, Howard Hughes Medical Institute, Seattle, WA.

Dr. Haohua Qian: University of Illinois at Chicago, College of Medicine, Chicago, IL.

Dr. Harris Ripps: University of Illinois at Chicago, College of Medicine, Chicago, IL.

Dedication

I would like to dedicate this work to the memory of my grandfather Andrew Redenti. It was through his constant encouragement and guidance that this accomplishment became possible.

For the support I have received from my entire family leading to the initiation and completion of my PhD. training, thank you.

Thank you, Dr. Lynne Chang for sharing all the things that make life a worthwhile challenge and adventure.

Table of Contents

Figures

Chapter 1

Introduction

1.1. Retinal Organization and Processing

The approximately 0.5 mm thick human retina is organized with three layers of neural cell bodies and two layers of synapses. Photoreceptor outer segments are most distal in contact with retinal pigment epithelium. Moving proximally one finds, the outer nuclear, outer plexiform, inner nucl ear, inner plexiform and ganglion cell layers. The average human retina contains 4.2 million cones and 92 million rods which synapse and converge onto 1 million ganglion cells (Curcio et al.,1990). In the dark, the primary vertical excitatory retinal transmitter glutamate is continuously released from photoreceptors into the ribbon synapse with horizontal and bipolar cells. This release is reduced by graded hyperpolarized potentials in photoreceptors in response to light stimulation. There are approximately nine neurotransmitter substances involved in retinal synaptic transmission (Vaney., 1990). Two major inhibitory transmitters present in lateral neural interactions in the retina by amacrine and horizontal cells are glycine and GABA (gamma-aminobutyric acid). At the second retinal synaptic layer some 11 types of bipolar cells communicate through a synaptic layer containing some 40 types of amacrine and 18 types of ganglion cells (Boycott et al., 1991; Vaney, 1990). Nitric oxide is one example of a neuromodulator which elevates cyclic GMP levels and increases calcium currents in photoreceptors (Goldstein et al., 1996). It is an objective of this dissertation to show that zinc is available and active as a neuromodulator enhancing the dynamic range of processing at the level of the outer-plexform layer.

1.2. Central Nervous System Zinc Physiology

Extensive research into the activity of zinc in brain tissue offers examples of zinc mechanisms potentially active in retinal tissue as well. Zinc-enriched neurons have been located in the entorhinal cortex, amygdala, and hippocampus of mouse and primate (Wenzel et al., 1997). Intracellular zinc modulates plasma membrane physiology, forms catalytic and structural subunits in approximately 300 zinc mettaloenzymes, and is bound to cysteine and histidine residues in most transcription factors (Grahn et al., 2001). It is well known that zinc homeostasis is essential for neural signaling and nuclear functioning (Dineley et al., 2003; Frederickson et al., 2000).

It has been estimated that zinc levels in the central nervous system are 200ng/mg protein (Dineley et al. 2003) and that approximately 95% of zinc in the CNS is bound by peptides and proteins (Frederickson et al., 2000). Intracellular stores of zinc can be taken up and released from mitochondria and metallothioneins (Sensi et al., 2004). In living cortical neurons, points of zinc entry include: voltage-gated Ca^{2+}channels, transporter-mediated exchange with intracellular Na^{+}, NMDA receptor-gated channels, and Ca^{2+} permeable channels gated by AMPA receptors.

In depolarized cortical neurons cytosolic concentrations of zinc range between 35 and 45 nM. (Sensi et al., 1997). Histochemically reactive, non-protein bound ionic zinc comprises, approximately 5% of CNS zinc (Frederickson et al., 2000). Vesicles of zinc enriched hippocampal terminals have zinc concentrations of up to 1.4mM and synaptic release is shown during depolarization (Frederickson et al., 2000).

Histochemical reactivity for zinc ions in neural tissue appears primarily in terminals containing glutamatergic vesicles (Wenzel et al., 1997). Recently, however, the

tyrosine hydroxylase positive post-synaptic superior cervical ganglions of mouse have demonstrated positive staining for zinc vesicular terminals as well (Wang et al., 2003). With zinc-rich glutamatergic and dopaminergic brain pathways well mapped, similar pathways are now being revealed in the retina.

1.3. Zinc Concentration in the Retina

Zinc is the most abundant trace metal in the retina (Miceli et al., 1999). In humans and rats retinal zinc levels are approximately 464 and 76 μg/g dry weight, respectively (Grahn et al., 2001). A decade ago, Wu et al. (1993) reported evidence of a dense band of ionic zinc in the region of the photoreceptor terminals of the tiger salamander retina. Subsequently, a high ionic zinc concentration was identified in a similar region near the base of the photoreceptors in the all-rod retina of the skate (Qian et al., 1997). A later study revealed zinc concentrated in photoreceptor outer segments of rats (Hirayama et al., 1990). More recently traces of zinc have been labeled in rat pigment epithelial cells, photoreceptor inner segments, outer nuclear, inner nuclear, outer plexiform, inner plexiform, and the ganglion cell layers (Akagi et al., 2001). Retinal pigment epithelial cells and photoreceptor inner segments have shown the strongest labeling for intracellular zinc (Akagi et al., 2001).

1.4. Zinc Function by Retinal Cell Type

1.4a. Retinal Pigment Epithelium

The retinal pigment epithelium (RPE) is situated between photoreceptor outer segments and the choroidal vasculature. The RPE reisomerizes retinol to 11-cis-retinal,

phagocytoses enormous numbers of shed photoreceptor outer segments, and aids in the absorption of scattered light (Strauss et al., 2005).

In humans the retinal pigment epithelial-choroid complex contains approximately 472 µg/g zinc (Grahn et al., 2001). In nonhuman primates, orally administered 65Zn was taken up and retained by RPE cells for up to 20 hours after administration (Newsome et al., 1992). Pigment epithelium zinc uptake and iris melanin content have been shown to correlate with age-related macular degeneration onset. Pigment epithelial tissue from blue and brown iris eyes was incubated in 100µM $ZnCl_2$ for 24 hours. Upon removal from high zinc culture, RPE from blue iris eyes showed no significant zinc increase, while brown iris RPE tissue showed zinc concentration factor increases of: 5.1 after 24 hrs., 4.4 after 3 days, and 2.8 after 7 days (Kokkinou et al. 2005). Fetal human retinal pigment epithelial cells cultured in low (250 nM) zinc, when compared to RPE in 11µM Zn culture, for one week exhibited the following decreases: zinc content (40%), proliferation (63%), catalase activity (68%), alkaline phosphatase activity (61%) and metallothionein (82%) (Tate et al., 1995).

Zinc incubation stimulates phagocytosis in RPE tissue as demonstrated in cultured human RPE cells. Those incubated in 25 µM $ZnCl_2$ overnight, exhibited greater rod outer segment uptake than RPE cells cultured in zinc-free medium (Miceli et al., 1994).

Bioavailable zinc regulates RPE zinc-mettalothionene levels by stimulating gene transcription and slowing protein degradation enhancing scavenging of free radicals. Human RPE cells cultured in 14µM $ZnCl_2$ for 24 hrs exhibit increased resistance to H_20_2 oxidative stress, higher mettalothionene and catalase levels when compared to control cells in 0.55µM $ZnCl_2$ (Tate et al. 1999).

In human donors aged 28-91, peripheral RPE contains higher concentrations of zinc-mettalothionene than macular RPE. Macular RPE from donors up to age 70 contained 17.6µg of cytosolic zinc-metalothionein, while RPE from those over 70 contained 5.6 µg. (Tate et al., 1993). It is possible that zinc deficiency and the consequential RPE oxidative damage, decreased phagocytosis, and decreased mettalothionene could be involved in the pathogenesis of age-related macular degeneration.

1.4b. Photoreceptor Outer Segments

The phototransduction cascade begins in the photoreceptor outer segment at the level of the rhodopsin molecule. Rhodopsin is a G-protein containing 11-cis chromophores which are isomerized by photons to all-trans retinal. The phototransduction second messenger cascade continues as metarhodopsin 2 activates transducin, activating cGMP phosphodiesterase which hydrolizes and closes cGMP gated Na+ channels, hyperpolarizing the photoreceptor cell. (Stryer 1991).

In rat ocular tissue photoreceptor cells contain the highest amount of zinc in the retina (Hirayama 1990). Analysis of the crystal structure of rhodopsin reveals the binding of seven zinc molecules, four of which occur in the intradisc space (Okada et al., 2002). Zinc binds to dark-adapted bovine rhodopsin in photoreceptor disks at a Kd of 2-10µM. In purified dark-adapted rhodopsin, zinc binding occurs at a Kd of 0.7µM. Zinc binding to purified dark-adapted rhodopsin reaches saturation at 20µM. Rhodospsin-zinc concentrations appear to increase during photo bleaching. Zinc binding to rhodopsin also exhibits a pH dependence which begins to increase at pH 6.0, reaches 50% binding at

pH 7.2 and increases to 100% binding at pH 8.2 (Terrence et al., 1992).

One functional role of zinc localized to outer segments appears to be modulation of rhodopsin thermal stability. In bovine rhodopsin solubilized in detergent, the thermal stability of rhodopsin is decreased with increasing zinc. At 55°C, thermal bleaching occurs at K rate constants of 0.028 +/- 0.002 min (0 µM Zn) and 0.056 +/- 0.003 min (50 µM Zn). The zinc-rhodopsin complex formed upon illumination results in a Meta 2 intermediate which decays faster, and a reduction in Meta 3 synthesis. With faster Meta 2 decay, opsin and free all-trans retinal may bypass the Meta 3 intermediate (Del Valle et al., 2003). Thus zinc appears to enhance rhodopsin activity.

Another function for outer segment zinc is the enhancement of rhodopsin phosphorylation. Bovine rod outer segments exposed to light showed zinc affecting the rhodopsin substrate enhancing phosphorylation, facilitating inactivation of active rhodopsin and its restoration to the dark (11-cis) state (Shuster et al., 1996).

Retinol-binding protein and zinc-metallo alcohol dehydrogenase levels decrease with zinc deficiency. Inadequate levels of zinc and zinc-mettalo alchohol dehydrogenase result in decreased conversion of retinol to retinal as well as decreased conversion of ethanol to ethyladehyde. Consequently, zinc deficiency is implicated in some forms of night blindness (Smith et al., 1980).

In a secondary step of the phototransduction cascade, zinc is involved in cGMP regulation. Purified retinal rod cGMP phosphodiesterase contains 3-4 g atoms zinc/mole. Two tightly bound zinc ions are required for the structural integrity of the catalytic subunit and additional free Zn^{2+} ions are required for enzymatic activity(He et al. , 2000).

Zinc is also required for an ATP-dependant rhodopsin kinase to quench the activity of light-activated cGMP phosphodiesterase (Shuster et al., 1988).

In the late stage of rhodospin activation, zinc is involved in ending the phototransduction response. The Recoverin protein requires the binding of Zn^{2+} to initiate the deactivation of rhodopsin through a Ca^{2+} dependant inhibition of rhodopsin kinase (Permyakov et al., 2003).

The Rim protein is a 220 kDa glycoprotein involved in the maintenance of photoreceptor outer segment morphology. Zinc enhances the structural integrity of outer segments by stabilizing nucleotide binding to the Rim protein (Shuster et al., 1988).

1.4c. Photoreceptor Inner Segments

Photoreceptor inner segments are essential for photoreceptor energy production and contain approximately 70% of retinal mitochondria. Inner segments are also the source of continuous disk production for outer segment regeneration.

In cultured mouse photoreceptors, zinc was shown to prevent reactive oxygen species production and to act as peroxide scavenger. The plasma membrane was protected in zinc incubated photoreceptors from oxidative damage. Zinc cultured cells demonstrated survival rates significantly higher than untreated cells. Oxidative stress induced apoptotic cell death which eliminated photoreceptors cultured in the absence of zinc. (Carmody et al. 1999).

1.4d. Photoreceptor Soma

A recent experiment has shown changes in localization of free zinc between dark and light adapted states. In sections of the dark-adapted rat retina a strong zinc concentration appears in photoreceptor soma. During light adaptation zinc in the soma no longer is visualizable and only photoreceptor outer segments exhibit a strong concentration of ionic zinc. (Ugarte et al., 1999).

A number of studies demonstrate evidence of zinc affecting photoreceptor conductances of different ion species. In salamander rod photoreceptors the noninactivating potassium current is slowed and its activation curve shifted towards positive potentials when zinc is added to the extracellular solution (Kourennyi et al., 2002). In isolated cones of tiger salamander, zinc inhibited the anion conductance through the synaptic terminal glutamate transporter. The presence of 26.5μM zinc was shown to cause a half-maximal reduction of currents evoked by 200 μM glutamate at -60mV (Spiridon et al., 1998). Incorporating the effect of zinc on the noninactivating potassium current, a computer modeled photoreceptor was developed with a faster activation of the light response and a broader frequency range (Kourennyi et al., 2002).

1.4e. Bipolar Cells

There are approximately eleven types of bipolar cells present in human retina. The rod bipolar cell receives synapses from 15-30 rod cells, while 10 forms of cone bipolar cells receive synapses from cone photoreceptors (Kolb, 1970). Off-center bipolar cells depolarize in response to photoreceptor glutamate release. On-center bipolar cells hyperpolarize upon photoreceptor glutamate exposure (Werblin 1991).

GABAA and GABAC receptors of isolated mouse bipolar cells demonstrate current inhibition in the presence of ionic zinc. Both GABAA and C receptor subtypes exhibited unique sensitivities to zinc. The GABAC receptor was more sensitive to zinc inhibition with an IC50 of 1.9 µM. Inhibition of the GABAA receptor required a higher zinc concentration with an IC50 of 67.4 µM (Kaneda et al, 2000). The kinetics of carp bipolar cell GABAA and GABAC receptors are altered byexposure to zinc. In cultures of isolated carp bipolar cells, micromole concentrations of zinc resulted in GABAC responses with slowed activation, slowed desensitization, and accelerated deactivation. In contrast GABAA receptors exposed to zinc responded with accelerated activation, accelerated desensitization, and no effect on deactivation (Han et al., 1999). It is plausible that zinc modulation of GABA receptors on populations of bipolar cells serves to refine transmitter signaling relative to lateral inhibition.

1.4f. Horizontal Cells

There are three types of primate horizontal cells. HI horizontal cells synapse with rods and long wavelength cones, HII cells synapse with short wavelength cones, and HII cells are thought to synapse with long wavelength cones. Each horizontal cell type responds to photoreceptor stimulation with hyperpolarizing responses (Ahnelt et al., 1994). In a center-surround organization coupled horizontal cells also respond to stimulation of neighboring receptive fields.

N-methyl-D-aspartate (NMDA) receptors are expressed on isolated catfish horizontal cells. The extracellular histidine residue of the NMDA channel binds zinc ions relative to extracellular pH. The IC50 for zinc inhibition if the NMDA current was

26.4μM at pH 7.4 and 86μM at pH 6.5. Higher zinc binding occurs closer to the free amino acid histidine pH 7.2 (Wu et al., 1996). It is at this histidine residue that zinc exerts its modulatory effect on the NMDA receptor.

The isolated catfish cone horizontal cell expresses GABAC receptors which gate chloride currents and are downmodulated by zinc. In control patch-clamp recordings, the half-activation concentration (IC50) of GABA was 2.99μM. In the presence of 10 μM zinc, the maximum GABA response was reduced to 60% and the GABA EC50 was increased to 17.32 μM. It is suggested that inhibition occurs as zinc binds to extracellular receptor sites. Thus, zinc released from photoreceptor terminals could modulate horizontal cell GABAC receptor activity (Dong et al., 1995).

The AMPA mediated currents of isolated adult hybrid striped bass horizontal cells, stimulated with 200μM glutamate, demonstrated inhibition in the presence of 3, 30, and 200μM zinc. Increasing zinc concentrations reduced whole-cell peak AMPA mediated currents by 2% 30% and 56% respectively In the presence of zinc, the glutamate induced half-maximal current EC50 rose from control levels of 50 +/- 3 to 70 +/ 6μM (Zhang et al., 2002).

In a recent study of L-type horizontal cell activity, zinc enhanced horizontal cell responses to low wavelength light stimulation. In isolated carp retina, dark-adapted L-type Horizontal cells exposed to 25μM Zn^{2+} exhibited enhanced sensitivity to 500 nm flashes and decreased sensitivity to 680 nm flashes. This differential modulation of L-type horizontal cell responses to red and blue wavelength stimuli is speculated to involve zinc modulation of GABA receptor activity, and photoreceptor glutamate release. (Dong et al., 2001).

1.4g. Amacrine Cells

There are forty morphologically distinct types of amacrine cells active as interneurons in the inner plexiform layer of humans. Amacrine cells are typically classified based on dendritic branching and IPL strata localization (Kolb et al., 1981).

In the mouse retina there are approximately 450 dopaminergic amacrine cells active in inner plexiform neuromodulation during light-adaptation. Isolated mouse dopaminergic amacrine cells exposed to GABA exhibit large inward chloride ion currents. The GABA evoked currents of dopaminergic amacrine cells are inhibited by zinc with an IC50 of 58.9 +/- 8.9μM (Feigenspan et al., 2000).

Zinc concentrations from 1-10μM potentiate glycine currents on amacrine and ganglion cells by modulating receptor affinity for glycine. As zinc concentrations approached 100μM the glycine currents became increasingly inhibited. All zinc concentrations inhibited GABAA activated currents of glycinergic amacrine cells (Li, et al., 1999).

Rat retinal glycinergic (AII) amacrine cells allow for the visualization of ionic zinc in their neural processes. Glycinergic currents of AII cells exhibit concentration-dependant zinc modulation, being enhanced by10μM and inhibited when exposed to concentrations of 50μM or more (Kaneda et al., 2005).

1.4h. Ganglion Cells

Ganglion cells receive signals from bipolar and amacrince cells as part of the most complex stage of retinal processing. In cat retina, approximately 50% of ganglion cells are categorized as Aplha or Beta type cells. Alpha ganglion cells are Off-center and

branch only in sublamina a. Beta ganglion cells are on-center and branch in sublamina b. The remaining 50% of ganglion cells fall into approximately 21 morphologically distinct subtypes (Kolb et al., 1981).

Goldfish retinal ganglion cells exhibit both K+ and Cl- currents at resting membrane potentials close to -80mV. In isolated goldfish ganglion cells under whole-cell recording, nanomolar levels of zinc activate a zinc-dependentprotein kinase C which decreases background Cl- current. (Tabata et al., 1999).

In isolated ganglion cells of the tiger salamander, 1µM zinc increased the peak amplitude of the ganglion cell response to 100 µM glycine from 750 pA to 1,300 pA. Low concentrations of zinc (<2µM) functioned allosterically to activate the fast-component glycine receptor induced Cl- currents, but had no effect on slow-component of glycine receptors, while zinc concentrations of 100µM decreased peak glycine responses by 63%. (Han et al., 1999).

Tiger salamander ganglion cells respond to NMDA exposure with an inward current which is blocked by 100 µM Zn^{2+}. In tiger salamander retinal slice preparations, currents induced by NMDA, kainate, and glutamate were blocked by the presence of 100µM zinc (Gottesman et al., 1992). Exogenous zinc can act allosterically to inhibit ganglion cell NMDA receptors preventing excessive calcium influx, reactive oxygen species production, and glutamate toxicity. Physiologically high (>50µM) levels of zinc can create reactive oxygen species through an ascorbate/iron mechanism (Ugarte et al., 1998).

1.4i. Mueller Radial Glial Cells

Mueller cells function as the primary glial cell of the retina. The distal villi of the Mueller cell contact photoreceptor outer segments forming the outer limiting membrane. The proximal endfeet of Mueller cells contact the basement membrane forming the inner limiting membrane.

Glutamate transporters of isolated tiger salamander Mueller cells demonstrate inhibition by zinc of the uptake and reverse of the uptake process. The IC50 of glutamate uptake blocking and inhibition by zinc was 66μM and <1μM, respectively. Zinc inhibition of glutamate transport occurred independent of voltage, on the extracellular surface, by decreasing the transporter's affinity for glutamate. Zinc enhanced activation of anion conductance of the glutamate transporter (Spiridon et al., 1998). In skate retinal Mueller cells, GABA A receptor currents elicited by 1μM GABA were enhanced by 10μM zinc (Qian et al., 1996).

1.5. Whole Retinal Zinc Function

1.5a. Neuroprotection

Zinc works as a retinal antioxidant by binding to the histidine residues of the copper-zinc superoxide dismutase and providing protein stability (Richardson et al., 1975). Copper-Zinc Superoxide dismutase is found at higher concentrations in the retina than in other ocular tissue where it catalyzes the dismutation of superoxide radicals to molecular oxygen and water.(Behndig et al., 1998).

In patients with age-related macular degeneration, there is a significant decrease in serum zinc, superoxide dismutase, and catalase (Wuet al., 1994). Patients with age-

related macular degeneration supplemented with 80mg zinc and other antioxidants show delayed progression of retinal degeneration (Age-Related Eye Disease Study Research Group, 2001).

The retina of Cynomolgus monkey models of early onset macular degeneration contain four times less zinc and consequently less metallothioneine, exhibiting more oxidative stress and increased levels of glyceraldehyde 3-phosphate dehydrogenase and albumin (Nicolas et al. 1996). Zinc supplementation in insulin-dependent diabetic patients results in decreased retinal lipid peroxidation (Faure et al. 1995). The antioxidant properties of ionic zinc and metalothione ine across studies appears essential for retinal health.

An increasing number of molecular pathways for zinc involvement in cell survival are being revealed. At least basal levels (~40nM) of cytosolic zinc are required for cell survival. Retinal cell cultures subjected to 24 hrs. of intracellular zinc depletion by TPEN chelation exhibited caspase dependant apoptotic death (Hyun et al. 2000). In cultured chick retinal neurons the pro- apoptotic binding of ^{125}I-NGF (ligand) to the $p75^{NTR}$ (receptor) was inhibited by 100µM zinc. Attenuation by zinc of this ligand-receptor cross linking provides a mechanism of apoptosis inhibition (Allington et al. 2001). Zinc also prevents apoptosis induced through glutamate toxicity. Cultured fetal rat retinas briefly exposed to glutamate or NMDA exhibited delayed cell death. In the presence of 3 to 30µM zinc, glutamate and NMDA-induced cell death was ameliorated (Kikuchi et al. 1995). It is predicted that zinc inhibits calcium uptake during glutamate overexposure thereby preventing initiation of the apoptotic cascade.

1.5b. Development

During development rats fed a zinc deficient diet produced fetuses from day 12-21 gestation with retinal folding, deficient optic cup invagination, and absent choroid fissure closure (Rogers et al., 1987). Release of synaptic zinc during post- natal days 1-24 has been shown to refine axons during remodeling of ganglion cell projections to the lateral geniculate nucleus (Land et al., 2001).

1.5c. Toxicity

During retinal ischemia zinc-accumulating neurons are injured. A significant number of retinal neurons died when exposed to 300-500μM Zn^{2+} in culture. Pyruvate protected against retinal cell ischemic zinc accumulation and death in vivo (Yoo et al., 2004).

1.6. Summary

The body of literature outlining the role of zinc in retinal physiology continues to grow. It is apparent that healthy retinal neurons require basal physiologic levels of zinc to survive. Each retinal layer exhibits cellular localization of zinc and each cell subtype demonstrates zinc sensitivity. Retinal pigment epithelial cells uptake zinc and increase their essential role of phagocytosis. Zinc ions are essential in the phototransduction cascade from inactive rhodopsin conformation to binding of recoverin to quench rhodopsin activity. At each plexiform layer zinc demonstrates its modulation of a number of excitatory and inhibitory receptors.

Chapter 2

Endogenous Zinc as a Neuromodulator in Vertebrate Retina: Evidence From the Retinal Slice

2.1. Skate Slice Introduction

Studies of the transretinal electroretinogram (ERG) of the skate (*Raja erinacia*) eyecup have provided evidence that endogenous zinc plays a role as a neuromodulator in vertebrate retina (Rosenstein, et al., 2001). With GABA receptor activity blocked by 200 mM picrotoxin, superfusion of the zinc chelating agent histidine (100 mM) increased by about 2-fold the ON (b wave) and OFF (d-wave) components of the ERG. In addition, as shown first in the salamander and skate retina (Wu, 1993; Qian et al., 1997), and more recently in mammalian retinas (Kaneda et al. 2001) an accumulation of ionic zinc has been localized to the base of the photoreceptors. These observations support the hypothesis that zinc, co released with glutamate from photoreceptor terminals, may serve as a neuromodulator in the outer plexiform layer of the vertebrate retina. If this is the case, one would expect to observe an effect of histidine application on the conductance of second-order cells in the retina of the skate.

2.1. Skate Slice Methods

Skates were obtained through the Marine Resources Center of the Marine Biological Laboratory (Woods Hole, MA). After approved euthanasia, the eyes were enucleated and dissected . The anterior portion of the eye, including cornea and lens, were removed and the eyecup flattened. The eyecup was placed retina side down onto a 0.22 micron pore membrane filter (Millipore) and sclera peeled away leaving retina attached. Retina on filter membrane was submerged under elasmobranch Ringer's solution 250 NaCl mM, 6 KCl mM, 1 $MgCl_2$ mM, 4 $CaCl_2$ mM, 360 urea mM, 10 glucose mM, and, 5 *N*-2-hydroxyethylpiperazine-*N*-2-ethanesulfonic acid (HEPES)

mM, titrated to pH 7.6 with NaOH) and sliced using a Stoelting tissue Chopper. Slices (200µm thick) from the all-rod retina of the skate were positioned on a glass slide and visualized using a fixed-stage microscope equipped with a water-immersion objective and Nomarski differential interference contrast optics. Whole-cell patch recordings were obtained under conditions of steady ambient illumination from horizontal cells of the inner nuclear layer, located below the base of the photoreceptors (Fig. 1A). Glass capillary electrodes, pulled to a resistance of 2 to 4 megohms, were filled with a standard skate internal solution (Qian et al., 1997) and the fluorescent dye, Lucifer yellow (0.3%). In addition, cesium chloride (204 mM) was added to suppress potassium currents. Holding potentials of -40 mV were used, thus avoiding the transient outward currents seen in these cells when they are held at more negative potentials (Malchow et al., 1990). The preparation was superfused with a continuous flow of skate-modified Ringer solution at approximately 1 ml per min. This could be rapidly exchanged with a Ringer solution to which histidine (100 or 500 mM) had been added. The higher concentration provided a faster increase in histidine concentration in the experimental chamber, but the ratios of the current increases measured were found to be independent of drug concentration.

2.2. Skate Slice Results

Responses to 10 ms steps in voltage (Fig. 1B) were obtained from horizontal cells like the one shown in the fluorescence micrograph of Figure 1C. Note the brightly stained terminals suggestive of the knob-like endings observed in sections of Golgi-stained skate external horizontal cells (Malchow et al. 1990). To monitor currents during solution changes, it was convenient to hold the cell at -40 mV and step the voltage to -120 mV.

Applying histidine (500 mM) for 2 min produced a 40% increase in the inward current as compared with that obtained in Ringer (Fig. 1B). Using a different protocol, in which the duration of the -120 mV step was 0.1 s, the time course of the current changes during 500 mM histidine applications and Ringer washes was measured and plotted (Fig. 1D). Each point represents the average of data from 3 successive steps, except for the "Ringer Control" points (square symbols) where 9 successive steps have been averaged. The initial increase in inward current observed in histidine approached saturation in less than 3 min. When the solution was returned to Ringer for a period of 5 min, 81% recovery was observed. A subsequent histidine application followed by Ringer wash gave comparable results. Data similar to that shown in Figure 1D were obtained from 6 horizontal cells, normalized to the current measured at V_C -120 mV in control Ringer solution, and averaged (Fig. 1E). The inward current increased 42% in histidine at V_C -120 mV; when returned to Ringer, the increase in current was reduced by 72%.

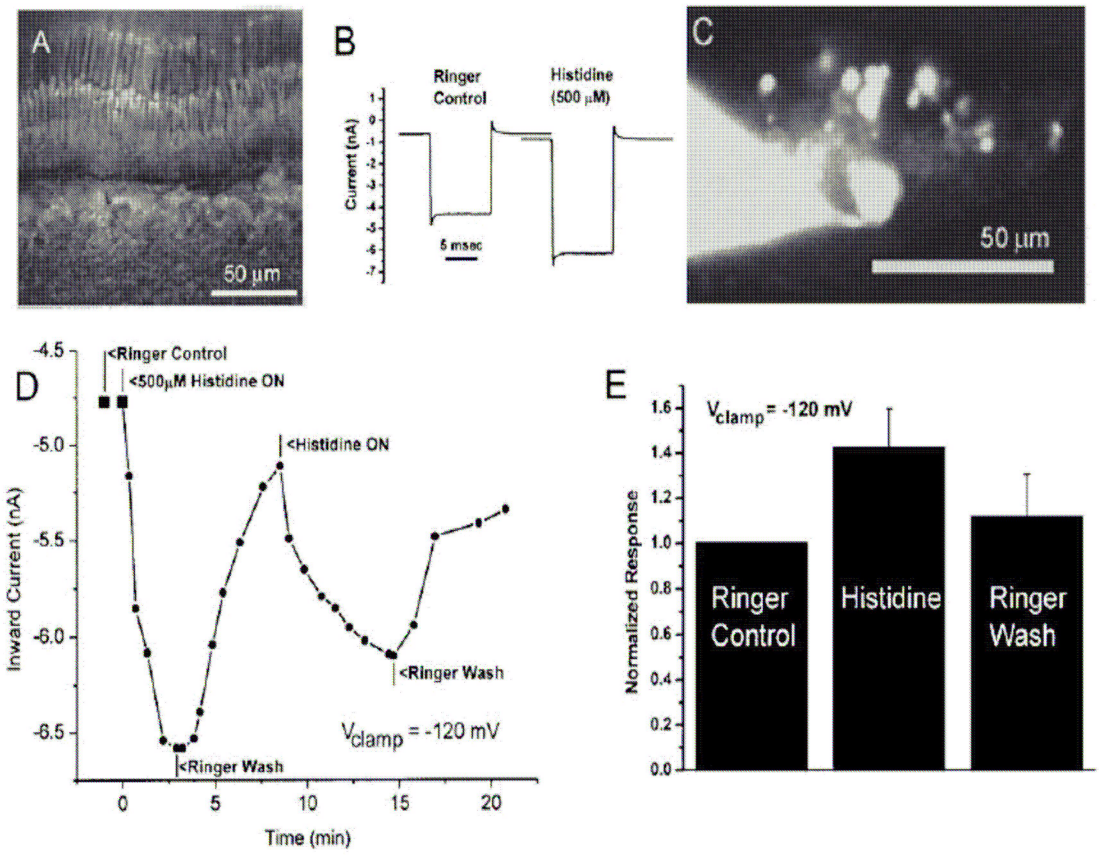

Figure 1. (A) Light micrograph of a 200µm retinal slice from skate retina. (B) Whole-cell voltage-clamp recordings from a skate horizontal cell during 10 ms steps from a holding potential of -40 mV to -120 mV in control Ringer solution and after 2 min in 500 mM histidine. (C) Fluorescence micrograph of a skate horizontal cell recorded and stained with Lucifer yellow in the retinal slice during whole-cell patch clamp. (D) Time course of horizontal cell conductance increase upon histidine application during a 100 ms step to a potential of V_C -120 mV from a V_C -40 mV holding potential represented by measured voltage-clamp inward currents. After a Ringer wash, the conductance recovers. (E) Horizontal cell currents measured in histidine (n=5) and subsequent Ringer wash (n =5) at V_C -120 mV normalized to current in control Ringer.

2.3. Skate Slice Discussion

Since the skate horizontal cell has no ligand-gated GABA receptors (Malchow et al.,1990) the well known effect of zinc on these receptors is not relevant (Wu et al., 1993). Glutamate receptors of skate horizontal cells have not been studied in this regard, but the possibility that zinc is acting directly on horizontal cells to reduce their permeability seems remote. Retinal horizontal cell glutamate receptors have been identified as AMPA and kainite receptors (Wu et al. 1998) although metabotropic glutamate receptors have been reported in one case (Gafka et al., 1999).

AMPA and kainite receptors studied on neurons elsewhere in the nervous system are generally enhanced by zinc at low concentrations (Bresink et al., 1996; Lin et al., 2001) Similar observations have been reported for retinal horizontal cells (Yang et al., 2001) but most studies have shown no effect of zinc on these cells (Wu et al., 1993; Schmidt, 1999; Shen, et al., 1999), with one exception, where currents were reduced (McMahon et al., 2001). For example, a zinc concentration of 50 µM, while high enough to block glutamate release from salamander photoreceptors, showed no effect on horizontal cell responses to applied glutamate (Wu et al., 1993). Similarly, it is important to note that, as a chelating agent, histidine, which has a much higher affinity for Zn^{2+} than for Ca^{2+} and is not membrane-permeable, would be expected to reduce, not increase, the ERG response if it were acting directly to reduce calcium entry needed for photoreceptor transmitter release (Rosenstein and Chappell, 2001). The skate horizontal cell can serve as a glutamate electrode, an increase in photoreceptor transmitter release will be reflected in an increase in horizontal cell conductance. With these considerations in mind, the increase in membrane conductance observed in the presence of histidine is

interpreted to represent an increase in photoreceptor transmitter release. This effect is predicted to be due to the chelation by histidine of endogenous zinc. Thus, in the presence of histidine, the inhibitory feedback process is suppressed, calcium entry into the receptor terminals is increased, and transmitter release is enhanced. This mechanism probably represents an important component of "neural" adaptation, comprising processes that are distinct from those governed directly by the bleaching and generation of rhodopsin (Dowling et al 1977; Green et al., 1975).

Chapter 3

Zinc Chelation Enhances the Zebrafish Electroretinogram b-wave

3.1. Zebrafish Electroretinogram Introduction

Earlier studies in isolated cells and eyecup of the skatepure -rod retina (*Raja erinacea*) support the notion of a role for endogenous zinc as a neuromodulator in the outer retina of vertebrates. Application of the zinc chelator histidine (100 µM) in the presence of the GABA-blocker picrotoxin (200 µM) doubled the amplitude of the skate electroretinogram (ERG) b-wave recorded in the skate eyecup preparation (Rosenstein et al. 2001). Consistent with this observation, the application of histidine to the skate retinal slice preparation resulted in a reversible increase in inward current from identified horizontal cells recorded in voltage clamp mode (Chappell and Redenti, 2001). Here we report results from an ERG study that is similar to the one in skate but uses the *in situ* eyecup preparation of the zebrafish, a vertebrate whose retina has both rods and cones.

3.2. Zebrafish Electroretinogram Methods

Adult zebrafish (*Danio rerio*) obtained from a colony maintained at the Marine Biological Laboratory, Woods Hole, Massachusetts, were anesthetized using 0.02% tricaine, immobilized with a 2 µL injection of 1% gallamine triethiodide (Flaxidil), and placed on their sides on a small sponge over a silver chloride pellet reference electrode. Their gills were irrigated with an oxygenated oral solution containing 2 g Instant Ocean per gallon distilled water (Westerfield, 2000). The cornea and lens were carefully removed to allow superfusion of the retina using a glass capillary manifold that could be switched from zebrafish Ringer (116 mM NaCl, 2.9 mM KCl, 1.8 mM CaCl2, and 5 mM HEPES) (Westerfield, 2000) to Ringer containing 200µM picrotoxin alone or 200 µM picrotoxin plus 100 µM histidine. All solutions were adjusted to pH 7.2. A glass capillary

agar bridge to another silver chloride pellet was placed in the eyecup as the recording electrode. Experiments were conducted in a darkened room in the presence of dim ambient illumination. ERG responses were recorded using a low-noise differential preamplifier (PAR113) having a bandpass of 0.03 Hz to 1 kHz, and stored with a DigiData 1200 acquisition system and pClamp6 software. The intensity of the unattenuated beam (log I =0) from a 100μW tungsten-halogen lamp operated at 8 amps from a dc-regulated power supply was 30 $\mu W/cm^2$ at the retina. ERG responses recorded from the zebrafish eyecup preparation following removal of the cornea and lens were generally smaller than those recorded using a corneal electrode on the intact eye, possibly due to trauma caused during the microsurgery. Thereafter, responses remained stable for up to an hour.

3.2. Zebrafish Electroretinogram Results

Figure 2A shows responses to 1.1 second flashes of intensity log I = -0.7. The b-wave component of the response (arrow) recorded during superfusion with Ringer (upper trace) was not significantly changed after 10 minutes in picrotoxin (middle trace). This suggests that GABAergic mechanisms do not have a large impact on the magnitude of the ERG b-wave in the zebrafish retina. The amplitude of the b-wave nearly doubled, however, within 30 min after the superfusate was switched to Ringer containing both histidine and picrotoxin (Fig.2A, lower trace). Note also the large apparent increase in the a-wave (photoreceptor potential), which is due probably to delayed onset of the b-wave as suggested by a 40% delay (50 ms ±13, n = 5) in b-wave time to peak in the histidine solution. Results obtained in response to 1.1 second flashes of intensity log I = -1 from

five zebrafish eyecup preparations, normalized to the response in picrotoxin, are illustrated in Figure 2B. After addition of histidine, b-wave amplitudes doubled (2.2 ± 0.4; mean ± SEM), while the average response in picrotoxin alone had been only slightly larger (by 0.12 ± 0.07) than the response in the control Ringer solution. Reversibility of the histidine enhancement of the b-wave response (log I = -1.7, normalized to the picrotoxin response at that intensity) is shown in Figure 2C. Note that a 20 minute wash in Ringer reversed the b-wave enhancement induced by 20 min in the histidine-containing test solution. The b-wave increased again when the histidine plus picrotoxin solution was reapplied for 10 minutes (not shown).

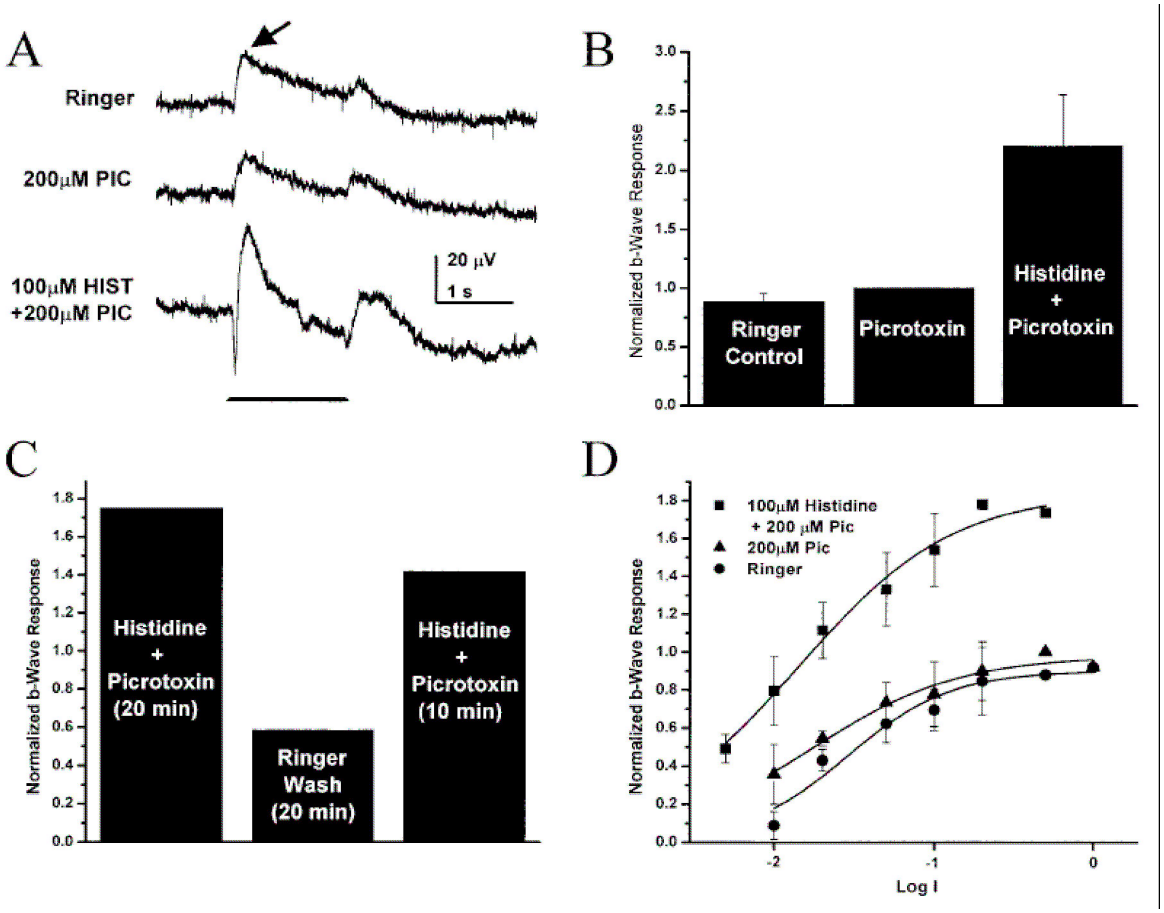

Figure 2. The zinc chelator histidine enhances the zebrafish ERG b-wave amplitude. (A) Adding histidine (HIST) nearly doubles b-wave amplitude of light response (bar = light ON, log I = -0.7) compared to Ringer with or without picrotoxin (PIC). (B) Normalized data at log I = -1 from five preparations. (C) Histidine-induced b-wave increment can be reversed and repeated by Ringer wash and reapplication of histidine-containing solution. (D) Intensity-response data from five preparations fitted by Naka-Rushton curves. Concentrations: 100 μM histidine, 200 μM picrotoxin.

3.3. Zebrafish Electroretinogram Discussion

The evidence of this study indicates that the effects of the zinc chelator histidine on the zebrafish retina, is similar to that observed in the all-rod retina of the skate. This electrophysiological evidence supports the hypothesis that zinc may be acting as a neuromodulator in the outer retina. The zebrafish retina contains both rod and cone afferent pathways. In light-adapted states, hyperpolarized rod cells release less transmitter and therefore less zinc. Low levels of available zinc during light-adapted states may then increase transmitter release by providing less inhibition of rod terminal calcium entry. During dark-adaptation, with cone receptors in a depolarized state, increased zinc release could inhibit Ca^{2+} terminal entry thereby conserving transmitter release.

Chapter 4

Zinc Chelation Enhances the Sensitivity of the Electroretinogram b-Wave in Dark-Adapted Skate Retina

4.1. Skate Electroretinogram Introduction

The retina of the skate remains an important model for studies in rod function and light sensitivity in the absence of cone pathways. In the skate, zinc regulates both GABA (Qian et al., 1997) and glutamate (Rosenstein and Chappell, 2003) receptors of isolated cells. Histidine is an amino acid endogenous in the retina, where it may play various roles in cell metabolism and disease (Wistow et al., 2002). Histidine can also increase the membrane currents recorded postsynaptically from horizontal cells during voltage-clamp in the skate retinal slice preparation (Chappell and Redenti, 2001). The effects of histidine support the notion that endogenous zinc may be playing a role in the physiological response of the retina to light. Histidine affected the zebrafish ERG by increasing the sensitivity of its duplex retina (Redenti and Chappell, 2002). This study supports previous investigations demonstrating that zinc chelation by histidine enhances the sensitivity of the b-wave of the ERG in an all-rod retina of the skate (Rosenstien and Chappell, 2003).

4.2. Skate Electroretinogram Methods

Skate were obtained through the Marine Resources Center of the Marine Biological Laboratory (Woods Hole, MA). The animals were allowed to dark-adapt for at least one hour prior to an experiment. After approved euthanasia, the eyes were enucleated and dissected under dim red light. The anterior portion of the eye, including cornea and lens, was removed; and the remaining retinal eyecup preparation was used for ERG recordings. Eyecups were placed into a chamber over a silver chloride reference electrode within a Faraday cage. The active silver chloride electrode was connected to

superfusion solutions in the eyecup via a glass capillary containing Ringer/agar. ERG responses to increasing intensities of illumination were recorded while the preparation was superfused (0.5 ml/min) with skate-modified Ringer's solution (Qian et al., 1997) alone, or to which 200 µM picrotoxin (to block GABAergic receptors in the retina known to be zinc-sensitive (Qian et al., 1997) and then 100 µM histidine plus 200 µM picrotoxin had been added. We had found that responses in picrotoxin did not increase after the first 10 min, but that ERG responses in histidine could continue to increase for up to 30 min. Therefore, the preparation was kept in the dark for 30 min in Ringer, at least 10 min in picrotoxin, and at least 30 min in histidine plus picrotoxin prior to recording an intensity-response series. One-second flashes were used to elicit ERG responses from which b-wave amplitudes were measured. The intensity of the unattenuated beam (Log I = 0) was 260 µW/cm2.

4.3. Skate Electroretinogram Results

Individual ERG responses recorded from one skate eyecup preparation in response to stimulation at an intensity of Log I = -3.0 are shown in Figure 3A. In addition to increased b-wave amplitude observed when picrotoxin, or histidine plus picrotoxin, were applied, an increased a-wave as well as a more prominent OFF component were often observed, as first reported by Chappell and Rosenstein (1996) from experiments using picrotoxin alone.

Similar data at all intensities were obtained from five preparations. Intensity-response data from one preparation are plotted in Figure 3B. A V_{max} under normal Ringer conditions for each eye was determined by obtaining the best fit of the Naka-Rushton

equation (Naka et al. 1996) to the intensity-response data obtained in the control Ringer solution. The value of V_{max} obtained was used to normalize the data before averaging it and plotting the results, which are shown in Figure 3C and 3D. Figure 3C is a bar graph of the averaged data from five preparations at the intensity Log I = -4, an intensity near the half amplitude intensity (σ) for the intensity response curve obtained in Ringer. The curves plotted with the intensity-response data in Figure 3D are the best fit of the data in Ringer, picrotoxin, and histidine plus picrotoxin, respectively, to the Naka-Rushton relation, using the least-squares approximation in Origin®. Using this approach, we could obtain the value of the intensity corresponding to the half amplitude (σ) of the Naka-Rushton curves, as well as the V_{max} for each of these curves. The values of V_{max} obtained increased from 0.95 in Ringer, to 1.09 in 200 μM picrotoxin, and 1.4 in 100 μM histidine plus 200 μM picrotoxin, while the values of (σ) shifted from a Log I of -4.3 to -4.52 and -5.13, respectively.

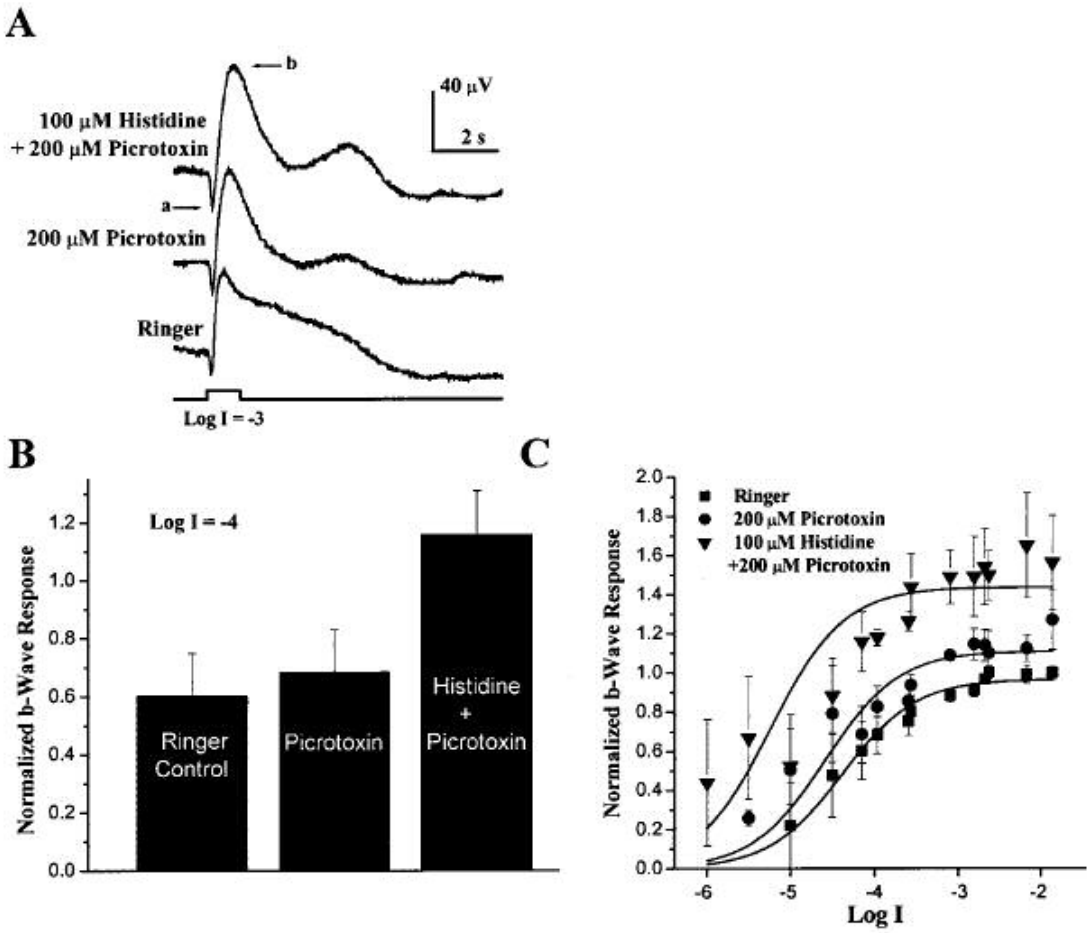

Figure 3. The zinc chelator histidine increases sensitivity of the skate electroretinogram (ERG) b-wave response. (A) ERG responses recorded from a dark-adapted skate eyecup preparation in response to a 1-s flash of white light at an intensity of Log I = - 3 (Unattenuated beam intensity, Log I = 0, was 260 µW/cm^2). The amplitude of the b-wave ("b", upper trace) of the ERG recorded from a dark-adapted skate eyecup preparation increased when 100 µM histidine (in the presence of 200 µM picrotoxin to block zinc-sensitive GABA receptors) was added to the superfusate. A small increase in the a-wave ("a", upper trace) was sometimes seen as well. (B) Normalized data at Log I = -4 from 5 preparations. (C) Intensity-response data, averaged and plotted (mean ± SEM),

with curves representing the best fit to the Naka-Rushton equation for each condition. The Log I of the half-amplitude intensity (σ) of these curves determined in Ringer, 200 μM picrotoxin, and in 100 μM histidine plus 200 μM picrotoxin were -4.3, -4.5, and -5.1, respectively. Thus, in addition to a 50% increase in V_{max}, σ for the histidine intensity-response curve was shifted 0.8 log units to the left, representing a 6-fold increase in sensitivity in the presence of histidine.

4.4. Skate ERG Discussion

The shift of (σ) toward dimmer intensities represents an increase in sensitivity of 0.8 log units (roughly a factor of 6) in the presence of histidine. Such an increase in sensitivity is consistent with the feedback model proposed by Wu et al. (1993) in which zinc feeds back onto photoreceptor terminals reducing Ca^{2+} entry and vesicular transmitter release. It would also be consistent with a reduced inhibition of glutamate receptors on second-order retinal neurons (Rosenstein et al., 2003) or possibly involve an effect of zinc on hemichannels (Chappell et al., 2003). Hemichannels have been suggested as a means of feedback from horizontal cells onto cones (Kamermans et al. 2001). The altered sensitivity in light response observed by chelation of extracellular zinc from the all rod retina, suggest an important neuromodulatory role for zinc in rod afferent pathways.

Chapter 5

Mouse Retinal Slice and Isolated Cell ZnT-3 Localization

5.1. Mouse ZnT-3 Introduction

The hydrophilic cation zinc cannot pass through membranes via passive diffusion and requires an active transport protein (Wang et al., 2003). In the central and peripheral nervous systems, co-localization of histochemically reactive zinc with the zinc transporter-3 (ZnT-3) protein has been shown on synaptic vesicles (Palmiter et al., 1996). The ZnT-3 protein is in the SLC30 family of transporters involved in ionic zinc homeostasis (Palmiter et al., 2004). The murine 388 amino acid ZnT-3 protein has six transmembrane domains and localizes primarily to membranes of zinc enriched terminal vesicles in neural tissue (Palmiter et al., 1996). The murine ZnT-3 gene has 8 exons and maps to chromosome 5 (Palmiter et al., 1996). In a murine knockout model, ZnT-3 was shown to be responsible for the sequestering and concentration of ionic zinc in mouse mossy fiber boutons of hippocampal neurons (Cole et al., 1999). Recent studies show increasing numbers of central and peripheral nervous system regions exhibiting colocalization of reactive zinc with the ZnT-3 protein (Danscher et al., 2003). In glutamatergic hippocampal mossy fiber pyramidal neurons, light and electron microscopy revealed a 60–80% co-localization of ionic zinc with the ZnT-3 protein on synaptic vesicles (Wenzel et al., 1997). In all levels of mouse spinal cord, ependymal cells of the central canal have shown antibody reactivity for the ZnT-3 protein (Danscher et al., 2003). Based on that study, (Danscher et al., 2003) proposed that the ZnT-3 protein in mouse spinal cord serves to regulate zinc homeostasis between cerebral spinal fluid and gray matter. It has been shown that the majority of ZnT-3 neurons are glutamatergic (Wenzel et al., 1997). Tyrosine hydroxylase positive post-synaptic superior cervical ganglions of mouse have recently been shown to contain zinc in vesicular terminals as

well (Wang et al., 2003). Approximately 5% of the somata and processes of these ganglia exhibit ZnT-3 protein antibody reactivity (Wang et al., 2003). To identify if the ZnT-3 protein is utilized to transport zinc in retinal tissue ZnT-3 localization in mouse retina was analyzed.

5.2. Retinal Slice ZnT-3 Localization Methods

Six male mice C57BL/6J (Taconic Labs) ages 12–18weeks were euthanized using carbon dioxide gas. The immunoperoxidase amplification protocol and ZnT-3 antibody used have been described (Wenzel et al., 1997). Modifications for retinal immunohistochemistry are described below. Palmiter et al. (1996) using Western blots of total cell proteins from control BHK cells and those transfected with constructs expressing ZnT-1, ZnT-2 or ZnT-3 showed that only the cells expressing ZnT-3 reacted with the ZnT-3 antibody, indicating that it does not react with the homologous proteins (Palmiter et al. 1996). Eyes were removed and placed in 4% paraformaldahyde in 0.1M sodium phosphate buffer (PBS), pH 7.4 for 4h at 4ºC. Eyes were then rinsed in PBS and cryoprotected, first in 10% sucrose for 1hr and second in 30% sucrose for 12hr, followed by further protection in frozen specimen embedding resin (Cryomatrix, Shandon) for 10–15min. Next, the eyes were placed in a cryostat and allowed to freeze for 30min at -20ºC. They were then transversely sectioned at 15–30 µm using a cryostat microtome (Bright Instruments). Sections (N = 42) were placed into 0.2ml PBS in 0.2–0.4ml chamber slide wells (Lab-Tek). The sections were rinsed 2x with PBS and then rinsed again 2x with 0.1M Tris.HCL buffer solutions (TBS) at pH 7.4. Endogenous peroxidases were inactivated through section incubation in 1.0% H2O2 in TBS for 2hr. Sections were then

incubated in a blocking buffer of 3% BSA, 3% goat serum, and 0.25% dimethyl sulfoxide in TBS (0.05M TBS/ 0.15M NaCl, pH 7.4) for 1hr. and rinsed for 15min 2x in TBS. Thereafter, the sections were incubated in an affinity-purified rabbit antibody specific for ZnT-3 diluted 1:20–1:100 in 2% BSA, 1% goat serum, and 0.25% dimethyl sulfoxide in TBS for 20–40hr at 4ºC. This was followed by rinse for 15min 4x in TBS. Sections were then incubated in biotinylated goat anti-rabbit IgG (Sigma) diluted 1:20–1:200 in 2% BSA, 1% goat serum, and 0.25% dimethyl sulfoxide in TBS for 24h at 4 ºC, rinsed for 15min 4x in TBS incubated in ABC (Elite ABC Kit: Vector Labs) diluted 1:200 in 2% BSA, 1% goat serum, and 0.25% dimethyl sulfoxide in TBS for 24h at 4ºC, and rinsed 2x in TBS pH 7.6. Finally, sections were incubated in DAB enhanced liquid substrate (Sigma) for 15min and then in fresh DAB for 5–10min followed by a rinse 2x in TBS pH 7.6 and a rinse 1x in PBS. Slides were covered and sealed for light microscopic analysis.

5.3. Retinal Slice ZnT-3 Results

Eight slices were processed for immunohistochemistry from each of six mouse eyes. Once successful parameters had been established, 42 of the 15–30µm slices incubated with ZnT-3 antibody showed a consistent robust reaction for protein localization. Antibody-labeled sections demonstrated elevated reactivity for the ZnT-3 protein in the photoreceptor inner segment region as well as in the outer plexiform, inner nuclear, inner plexiform, and ganglion cell layers (Fig. 4). Control retinal slices processed in the absence of the ZnT-3 antibody showed no distinct staining (Fig. 4, inset). The regions of the outer nuclear layer and the outer segments of photoreceptors showed no

ZnT-3 reactivity. The horizontal, bipolar, and amacrine somata regions of the inner nuclear layer showed consistent ZnT-3 reactivity slightly weaker than the reactivity in the region of inner segments. The inner plexiform layer, the synaptic region of amacrine, bipolar, and ganglion cells, demonstrated moderate reactivity for the ZnT-3 protein. The ganglion cell layer and inner limiting membranem region showed ZnT-3 reactivity with slightly more intensity than either of the plexiform layers. These observations were confirmed through more detailed examination at higher magnification (Fig. 5). We also observed that the proximal region of the inner nuclear layer where amacrine cell bodies predominate showed stronger immunoreactivity than the more distal region. Wang et al. (2003) reported the presence of ZnT-3 protein in superior cervical ganglia synapses containing tyrosine hydroxylase positive vesicles so that association of ZnT-3 protein with the small population of mouse dopaminergic amacrine cells should be considered in addition to the usual association of ZnT-3 with glutamatergic pathways. Although most cell bodies in the ganglion cell layer demonstrated strong labeling, it appeared that a small number of cells in this region were not immunoreactive for the ZnT-3 antibody.

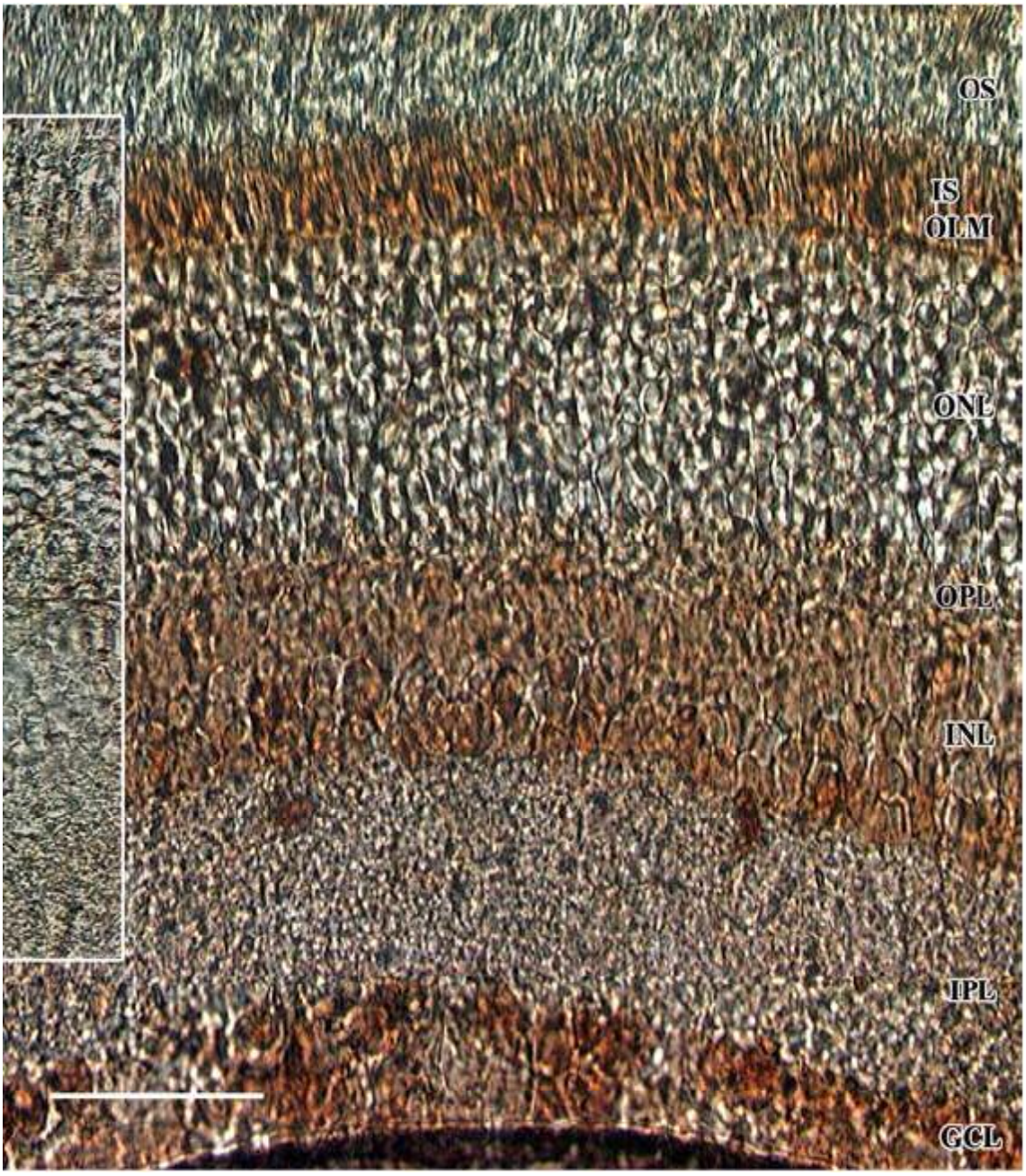

Figure 4. Mouse retinal ZnT-3 localization. The 40x light microscopic image shows a ganglion cell layer (GCL) with dark reactivity for ZnT-3 protein. The inner plexiform layer (IPL) shows weak granular reactivity. The inner nuclear layer (INL) soma and outer

plexiform layer (OPL) region of synaptic junctions present moderate levels of ZnT-3 reactivity. The outer nuclear layer (ONL) remains clear of reactivity. The inner segments and outer limiting membrane region (IS, OLM) show strong reactivity. Outer segments (OS) were clear of reactivity. The left inset is a control slice processed in absence of antibody. Bar: 50µm.

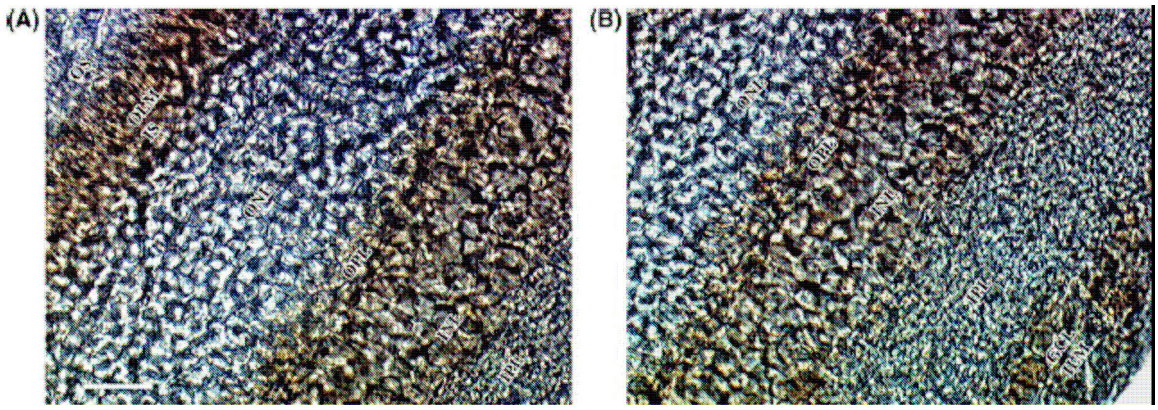

Figure 5. Mouse outer and inner retinal layer ZnT-3 localization. The 60x light microscopic images confirm the pattern of ZnT-3 localization consistent with that observed at lower power. (A) Outer retina: Inner segments and outer limiting membrane region (IS, OLM) show strong ZnT-3 localization. Photoreceptor outer segments (OS) and outer nuclear layer (ONL) soma remained completely clear of reactivity. The outer plexiform layer (OPL) synaptic region showed reactivity. (B) Inner retina: The inner nuclear layer (INL) shows reactivity. The inner plexiform layer (IPL) exhibited weak granular reactivity. The ganglion cell layer and inner limiting membrane region (GCL, ILM) show consistent reactivity. Bar:20µm. (Note that tissue orientation is approximately 45º with respect to that in Figure 4.)

5.4. Isolated Cell ZnT-3 Localization Methods

Poly-L-lysine treated slide covers were plated with 200µl of Ringer's solution [in mM] NaCl [137], KCl [5], $CaCl_2$ [2], $MgSO_4$ [1], Na_2HPO_4 [1], HEPES [10], Glucose [22], pH 7.4. Six adult C57BL\6 mice and four Long Evans rats were euthanized. Their eyes were removed and placed in ice-cold Ringer's solution. By cutting along the ora serrata with a microscissor, the cornea and lens were removed. Eyecups were submerged in Ringer solution and retinas were teased out of the eyecups with forceps. Retinas were then rotated slowly for 1hr in 35x10mm dishes containing: papain (2mg/ml) and L-cysteine (1mg/ml) in 3ml of Ringer's solution. Using a sterile 10ml glass pipette retinas were transferred to a 15ml tube containing 3ml of fresh Ringer's solution and rinsed 8x. Cells were then isolated by repeating 8x triturations, up to 64x, and plating 2-3 drops of supernatant onto treated slide covers. From each dissociated retina 10 slide covers of isolated cells were prepared for labeling. Cells were allowed to settle for 1hr and then fixed with 4% parafolmaldehyde. Cells were rinsed 3x with 0.1M PBS, pH 7.4. The cells were then rinsed with 0.6% Brij-58 for 20 min and rinsed in PBS 3x. Next, cells were rinsed in 0.05 M Tris-HCl buffer, pH 7.4, 2x. Cells were incubated in blocking buffer in TBS containing 3% BSA, 3% Goat Serum, 0.025% DMSO for 1hr, then rinsed for 10min 3x in TBS. Cells were then incubated in affinity purified rabbit anti mouse ZnT-3 antibody at concentrations of 1:20-1:100 for 1hr and rinsed with TBS 10min 4x. Next, mouse cells were incubated in goat anti-rabbit FITC label for 1hr and rat cells were incubated in biotynylated goat anti-rabbit for 6hrs. Rat cells were then incubated in ABC for 6 hours, rinsed, and incubated in 3,3'-diaminodenzidine for 10min. Finally, cells were

rinsed for 10 min 3x in TBS and for 10 min 2x in PBS. Slide covers were sealed to slides and cells imaged using light and confocal microscopy.

5.5. Isolated Cell ZnT-3 Results

Of the retinal cell types studied, only Mueller cells showed significant labeling for the ZnT-3 antibody. In each slide with visible antibody reactivity, 6-8 labeled Mueller cells were identifiable. In the majority of rat Mueller cells the protein localizations appeared significantly denser in the apical villi and endfeet regions (Fig. 6A). Other processes and somas of Mueller cells showed labeling with slightly lower concentration and intensity. In a preliminary mouse slice ZnT-3 study, antibody banding appeared primarily in regions in which Mueller cell apical villi, soma, and endfeet are found. Inner plexiform regions exhibited weak granular labeling which appeared to be due to densities at synaptic junctions. In this study it appears that the ZnT-3 protein is expressed throughout the Mueller cell. Using confocal three-dimensional reconstruction (Fig. 6B), mouse Mueller cells exhibited label ubiquitously. This seems to indicate that ZnT-3 may be used in a novel way as a zinc transporter by Mueller cells.

Bipolar cell, rod and cone soma treated under the identical labeling protocol, as Mueller cells exhibited no ZnT-3 localization. Presumptive photoreceptor cells were identified by small 3-4μm diameter soma and highly abundant distribution (Fig. 7C, D) (Koulen et al., 1999). Bipolar cell soma and processes also appeared clear of ZnT-3 reactivity (Fig. 7A,B). Other retinal neurons with indistinct morphology appeared less often and exhibited no reactivity.

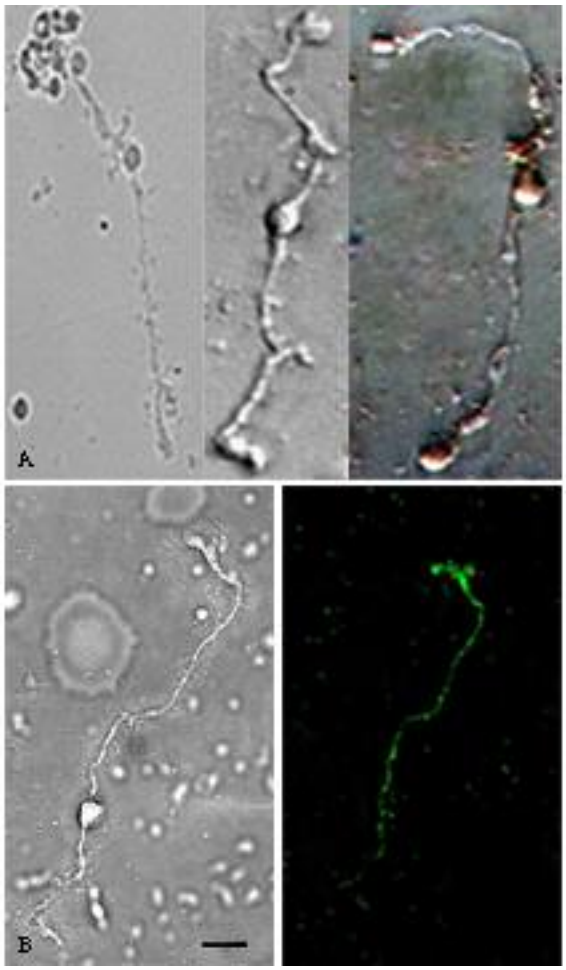

Figure 6. A: DAB labeled ZnT-3 isolated Rat Mueller cells under light microscopic analysis. Left/Center: control rat Mueller cells processed in the absence of the ZnT-3 antibody. Right: ZnT-3-DAB labeled Mueller cell viewed using conventional light microscopy. Mueller cell apical villi, soma, and endfeet appear to darkly label for the ZnT-3 protein, while process labeling is less visible. B: FITC labeled ZnT-3 localization of mouse Mueller cell using confocal microscopy. Left: white light. Right: fluorescent FITC. The ZnT-3 protein appears to be distributed ubiquitously in Mueller cells viewed here. Slightly higher concentrations of fluorescent label appeared in endfoot and apical regions.

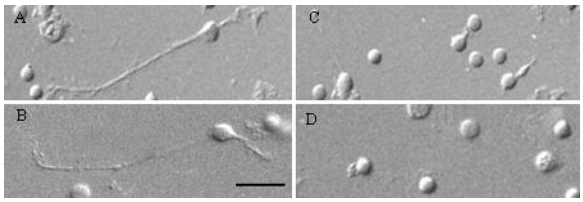

Figure 7. FITC labeled ZnT-3 incubated isolated mouse bipolar cells and photoreceptor somas showed no reactivity. A and B. Isolated bipolar cells incubated in ZnT-3 antibody showed no label. C and D. Presumed photoreceptor somas appear in abundance and were completely absent of ZnT-3 antibody label. When viewed using FITC fluorescence under the same conditions as those of Figure 6C, no ZnT-3 label was visible in these cells.

5.6. ZnT-3 Discussion

In general, ZnT-3 reactivity was found in regions of the mouse retina which have been found reactive for ionic zinc in prior studies of murine retinas as described above (Ugarte et al., 2001). This is consistent with the possibility that ZnT-3 mediated zinc transport may be related to zinc retinal neuromodulation as suggested by a number of studies. Already, a variety of vertebrate retinal cells have demonstrated zinc sensitivity. Relevant to ZnT-3 localization, Mueller cell GABAA receptor currents have been shown to increase when 10μM zinc and 1μM GABA are co applied under voltage-clamp conditions compared with GABA application alone (Qian et al., 1996).

It appears that localized retinal ZnT-3 may be involved in ionic zinc sequestering and vesicular storage in both plexiform layers. The ZnT-3 protein in the outer plexiform layer is co-localized in a region of zinc reactivity associated with glutamate in photoreceptor synaptic vesicles. Similarly, ZnT-3 is localized in the inner plexiform layer, the region of synaptic interaction among bipolar, amacrine, and ganglion cell processes. It is possible that AII cells shown to contain zinc in their processes, may co-localize ZnT-3 (Kaneda et al., 2005). The localization of ZnT-3 observed in several retinal layers suggests ionic zinc transport and localization may be a factor in normal functioning of the neural retina.

The localization of ZnT-3 immunoreactivity in the region of the photoreceptor inner segments and outer limiting membrane is of special interest. This is not a region of synaptic activity where synaptic vesicles are known to be concentrated. It coincides, however, with the location of a dense band of zinc found in other studies for light-adapted, but not dark-adapted, murine retinas (Ugarte et al., 1999). Rhodopsin and cGMP

phosphodiesterase utilize zinc in outer segments (Palsgard, et al., 2001). It has also been proposed that in the light adapted outer retina, higher amounts of zinc localize to an organelle (Palsgard et al., 2001). Approximately 60–75% of mouse retinal mitochondria can be found in photoreceptor inner segments (Perkins et al., 2003). Photoreceptor mitochondrial respiration has been shown to decrease in light-adapted retina (Perkins et al., 2003) and it has been shown that zinc inhibits mitochondrial ATP production (Perkins et al., 2003). In addition, zinc interferes with mitochondrial glycolysis, the tricarboxcylic acid cycle, and electron transport (Perkins et al., 2003). Consequently, in light-adapted inner segments, ZnT-3 transported zinc may have a functional significance relative to mitochondrial respiration.

Mueller cells project apical villi in the region of the photoreceptor inner segments where ZnT-3 protein is localized. We suggest the possibility that the Mueller cell apical villi in the region of the photoreceptor inner segments and the outer limiting membrane may utilize the ZnT-3 protein to regulate zinc homeostasis. Mammalian Mueller cells have already been shown to regulate extracelluler K+, glutamate and GABA in the neural retina (Reichenbach et al., 1997). It seems possible that ZnT-3 transporter associated with Mueller cells may be involved in zinc distribution in light and dark adapted states. Mueller cell associated ZnT-3 transporter could also account for the distribution of weak ZnT-3 immunoreactivity throughout the neural retina except for the region of the photoreceptor outer segments which are free of Mueller cell processes. If so, the Mueller cells may also provide a system for zinc homeostasis throughout the neural retina.

Chapter 6

Intracellular Zinc Localization in the Rat Retinal Slice

6.1. Intracellular Zinc Localization Introduction

A number of earlier studies have imaged intracellular retinal zinc in fixed tissue (Akagi et al. 2001; Ugarte et al., 1999; Qian et al., 1997) The fixed tissue studies utilized a Timm's silver amplification method. As mentioned previously, Akagi (2001) showed in fixed rat tissue intracellular retinal zinc in every cellular layer. Qian et al., (1997) showed a band of zinc in fixed skate retina only in the region of the outer plexiform layer. Osborne et al (1999) showed zinc only in photoreceptor soma in dark-adapted rat retinal tissue and a band of zinc only in outer segments in fixed light adapted tissue. It is apparent that intracellular bioavailable zinc varies with changes in physiologic states. The objective of this study was to visualize zinc in living light-adapted rat retinal slices using the intracellular zinc probe Zynpyr-1(Neurobiotex, TX).

6.2. Rat retinal Slice Intracellular Zinc Methods

Adult female Long Evans rats were euthanized using carbon dioxide gas. Eyes were removed and placed into ice-cold rat Ringer bubbled with 95% O_2 - 5% CO_2 using a plastic pipette tip. The rat Ringer used had the composition (in mM) of 124 NaCl, 1.75 KCL, 1.3 $MgSO_4$, 2.4 $CaCl_2$, 1.25 KH_2PO_4, 26 $NaHCO_3$, and 10 dextrose in double deionized H_20 at pH 7.4. Using microscissors anterior segment was cut away at ora serrata and the vitreous body removed. Four radial cuts were made into the posterior segment containing retina and the eyecup was flattened under saline. The flattened eyecup with retina was placed between two 13 mm diameter membrane filters.

Filter papers were gently separated using forceps resulting in isolated retina attached one filter and Choroid, RPE, and sclera attached to the other. Slices were made at 200µm

intervals with a Stoelting tissue chopper. Slices were then allowed to recover in oxygenated standard solution for 1hr at 32ºC. Slices were incubated in the intracellular zinc probe Zynpyr-1 at 25µM in Standard solution for 1 hour at 32ºC. Slices were rinsed four times to with Standard Ringer solution and imaged using an Olympus BX50WI fluorescent microscope.

6.3. Intracellular Zinc Localization Results

This study yielded results not previously seen in fixed tissue zinc localization studies. The weakest regions labeling for intracellular zinc using Zynpyr-1 were the inner plexiform and outer plexiform layers. The ganglion cell layer labeled with a moderate level of fluorescence in regions containing both soma and processes. The regions most intensely labeled were photoreceptor outer segments (Figure 8B). These regions exhibited a fluorescence approximately 2x greater than either plexiform layer.

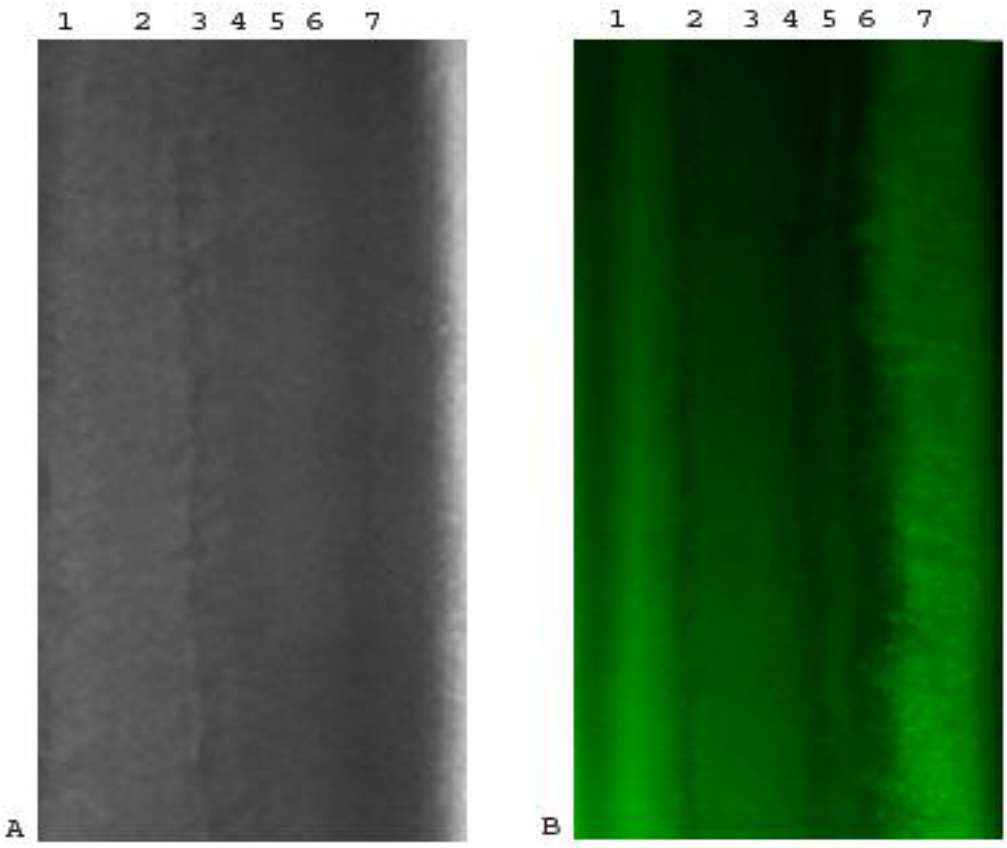

Figure 8. Intracellular Zinc Localization**.** (A) Long Evans rat retinal slice (200µ) incubated in 25µM Zynpyr-1 rinsed and placed in fresh saline for (20X) imaged under white light. From left to right: (1)ganglion cell layer , (2)inner plexiform layer, (3)inner nuclear layer, (4)outer plexiform layer, (5)outer nuclear layer, (6)inner segments, and (7)outer segments. (B) Same slice under 505/535 nm excitation/emission fluorescence. Retinal regions exhibiting intracellular zinc fluorescence from highest to lowest intensity: photorecepotor outer segments, ganglion cell layer, outer plexifiorm, and inner plexiform layer. Ionic zinc was not visible in either the inner nuclear or outer nuclear layer.

6.3. Intracellular Zinc Localization Discussion

As expected from previous studies in fixed tissue, both the inner and outer plexiform layers of the living light-adapted retina labeled for intracellular zinc. This could indicate that ionic zinc is available for synaptic release for neuromodulation during depolarization or neural processing. Under light-adapted conditions retinal neurons should be in a slightly hyperpolarized state resulting in less transmitter and or intracellular zinc externalization from synaptic regions. The ganglion cell soma and processes were strongly labeled and could possibly contain higher levels of intracellular zinc by passage of zinc ions through NMDA channels. In the photoreceptor outer segments a strong intracellular zinc concentration can be correlated to rhodopsin binding and second-messengers in the phototransduction cascade. During light-adaptation rhodopsin changes from its 11-cis to all-trans state. In the process of comformational change a number of the seven zinc ions known to be bound to the rhodopsin protein may be released into the interdisk space of the outer segments.

Chapter 7

Neuroimaging of Zinc Released by Depolarization of Rat Retinal Cells

7.1. Zinc Release Introduction

Ionic zinc (Zn^{2+}) is suggested to play a role as a retinal neuromodulator via its vesicular release from glutamatergic neurons (Wu et al 1993). As discussed previously, histochemical evidence from fixed retinal tissue has shown a band of reactive (ionic) zinc in the outer retina in a number of vertebrate species. Although its mechanisms of action remain elusive, ioniczinc play s an important role throughout the vertebrate nervous system and has been shown to be released from rat hippocampul tissue in a Ca^{2+} dependant manner. Hippocampul synaptic zinc concentrations have been measured in the range of 12-300 µM (Frederickson et al., 2000).

An important criterion to the vesicular release hypothesis for retinal zinc is demonstration of Zn^{2+} release in response to depolarization of retinal cells. Zinc sensitive fluorescent dyes provide the possibility to obtain evidence for release of endogenous zinc by neuroimaging of changes in extracellular zinc concentration resulting from depolarization of retinal neurons. This study provides evidence that the fluorescence of the zinc-sensitive, membrane-impermeable dye Newport Green was significantly enhanced by potassium-induced depolarization of retinal neurons. Fluorescence increases observed and quantified using microfluorescence techniques revealed the greatest increases in the outer plexiform layer and photoreceptor inner segment regions of living rat retinal slices.

7.2. Rat Retinal Slice Zinc Release Methods

Adult female Long Evans rats were euthanized using carbon dioxide gas. Eyes were removed and placed into ice-cold rat Ringer bubbled with 95% O_2 - 5% CO_2 using

a plastic pipette tip. The rat Ringer used had the composition (in mM) of 124 NaCl, 1.75 KCL, 1.3 $MgSO_4$, 2.4 $CaCl_2$, 1.25 KH_2PO_4, 26 $NaHCO_3$, and 10 dextrose in double deionized H_20 at pH 7.4 and was stored in plastic Falcon tubes. Eyes were cut along the ora serrata and the cornea, lens, and vitreous removed. Under Ringer solution, after making four short radial cuts from the edge of the eyecup, the eyecup was flattened and retina attached to membrane filter paper (0.2 µm, Gelman Sciences). Retinas were sliced at 200 µm (Stoelting tissue chopper) and transferred to individual sterile plastic slide wells containing 400 µl Ringer. Slices were allowed to recover for 1 hour under constant Ringer perfusion following sectioning. To avoid contamination, the microscope objective was coated with fresh saran wrap before each slice was observed. Slices were then imaged using an Olympus BX50WI microscope and images acquired using Metamorph software (Universal Imaging Corp). Slices were then incubated with 20 µM of the membrane impermeable form of the Zn^{2+} sensitive fluorescent dye Newport Green dipotassium salt (Molecular Probes). Images were taken at excitation/emission of 505/535 nm wavelengths to reveal basal efflux of extracellular Zn^{2+}. To induce retinal depolarization and stimulate Zn^{2+} efflux, retinal slices were exposed to 50 mM KCL in saline. Images of increasing extracellular fluorescence were then recorded and results quantified using the Metamorph software.

7.3. Zinc Release Results

Prior studies have used a modified Timm's method to identify the location of reactive zinc in fixed retinal tissue. Here microfluorescence techniques were used to image the extracellular release of reactive zinc (Zn^{2+}) from living rat retinal slices

maintained in Ringer's solution. A micrograph of one such slice as it appears when illuminated in white light is shown in the Fig. 9A. The same slice bathed in Ringer solution containing the membrane impermeable form of the Zn^{2+} sensitive dye Newport Green (12 μM) is shown in Fig. (9B as it appears when excited using incident light of 490 nm wavelength and observed at 520 nm. Within 2 minutes after the depolarization of retinal neurons by application of 50 mM KCl, more intense green bands become apparent in the region of the outer plexiform layer (OPL) and the photoreceptor inner segments (IS)(Fig. 9C).

In order to quantify the intensity changes of the zinc sensitive dye, the time course of changes in average pixel intensity for each region of the retina for one such slice were measured as shown in Fig. 10. When retinal cells were depolarized by the application of 50 mM KCl (arrow at 6 min) there was an immediate increase in fluorescence of the Zn^{2+} sensitive Newport Green across the retina. Within 8 minutes, the intensity of the outer retinal regions had increased by 80 to 90%. The intensity of all regions of the retina increased over 50%, possibly due to diffusion from the regions of the photoreceptor inner segments and the outer plexiform layer.

We monitored intensity changes in the region of the outer plexiform layer for ten different rat retinal slice preparations. For five of these, the 50 mM KCl was added 2 minutes after the Newport Green (Fig. 11, left arrow, squares). As a control, the 50 mM KCl was applied 10 minutes after the application of Newport Green for the other five preparations (Fig. 11, right arrow, circles) to compare basal levels of Zn^{2+} release from 2 minutes to 8 minutes without high KCl as well as to demonstrate that the depolarization-induced zinc release remained viable (at 10 min) in the control preparations. In each

case, the intensity of Newport Green fluorescence in the region of the outer plexiform layer increased immediately after application of 50 mM KCl with an increase of ~80% or more within a few minutes.

Using the Newport Green dissociation constant (Kd = 1 μM) for Zn^{2+} for the membrane-impermeable form of the dye provided by Molecular Probes®, it is possible to estimate the order of magnitude of the zinc concentration reached following zinc release. This can be accomplished using the relationship $[Zn^{2+}] = Kd (F - Fmin)/(Fmax - F)$, where F is the measured fluorescence intensity and Fmin and Fmax are obtained in the absence of Zn^{2+} and in the presence of a concentration of Zn^{2+} sufficient to result in dye saturation, respectively (Li et al., 2001). Measurements of Newport Green fluorescence alone and in the presence of 1 mM Zn^{2+}, a concentration sufficient to saturate the dye, provided pixel intensity values respectively of Fmin = 300 and Fmax = 4095. Based on the results from 8 preparations, this equation was used to estimate a mean concentration of Zn^{2+} in the region of the outer plexiform layer of 1.06 ± 0.25 μM (mean ± SEM) after 10 min in 50 mM KCl. Using this value in the same equation, the 80% increase in Newport Green dye intensity described above corresponds to an increase in Zn2+ concentration of over 200% after KCl application. Recent studies by (Li, et al., 2001) have shown that detection of Zn2+ by Newport Green fluorescence was not significantly affected by the presence of physiological levels of Ca2+ (2.4 mM) or Mg^{2+} (1.3 mM). Furthermore, they showed that up to 1 mM Ca2+ or Mg^{2+}, in the absence of Zn^{2+}, has little effect on the Newport Green dye fluorescence emission. The results reported here provide the first direct demonstration of Zn^{2+} release by depolarization of retinal cells.

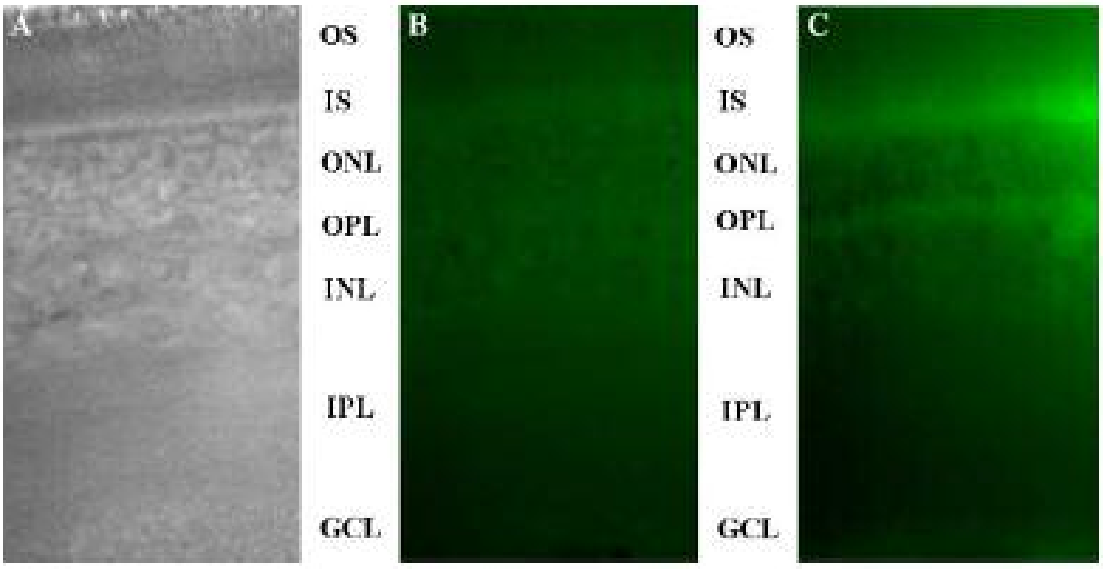

Figure 9. Zinc release by depolarization of retinal cells. (A) Two hundred micrometer thick living rat retinal slice in Ringer imaged under white light. Labels indicate the regions of the outer segments (OS), inner segments (IS), outer nuclear layer (ONL), outer plexiform layer (OPL), inner nuclear layer (INL), inner plexiform layer (IPL), and ganglion cell layer (GCL). (B) The same slice superfused with 12µM Newport Green added to Ringer imaged under 505/535 nm excitation/emission. Faint bands of fluorescence observed in the regions of the inner segments and outer plexiform layers are not obvious in the micrograph. (C) Bands of Newport Green Zn2+ fluorescence appear in regions of the photoreceptor IS and OPL 2 min following depolarization of retinal neurons by application of 50 mM KCl.

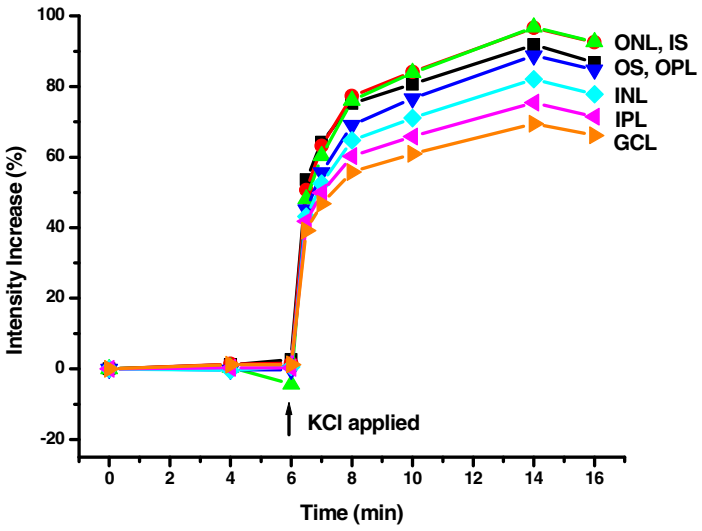

Figure 10. Newport Green intensity increase by region of a rat retinal slice. Depolarization of retinal cells by application of 50 mM KCl (arrow at 6 min) resulted in a substantial increase in fluorescence of the membrane-impermeable form of the Zn2+ sensitive dye Newport Green within 1 min. The increase, plotted as a percent of average pixel intensity for each region of the retina 6 min prior to KCl application, was largest in the distal retina, from the outer plexiform layer (OPL, downward triangles) to the outer nuclear layer (ONL, circles) and photoreceptor inner segments (IS, upward triangles).

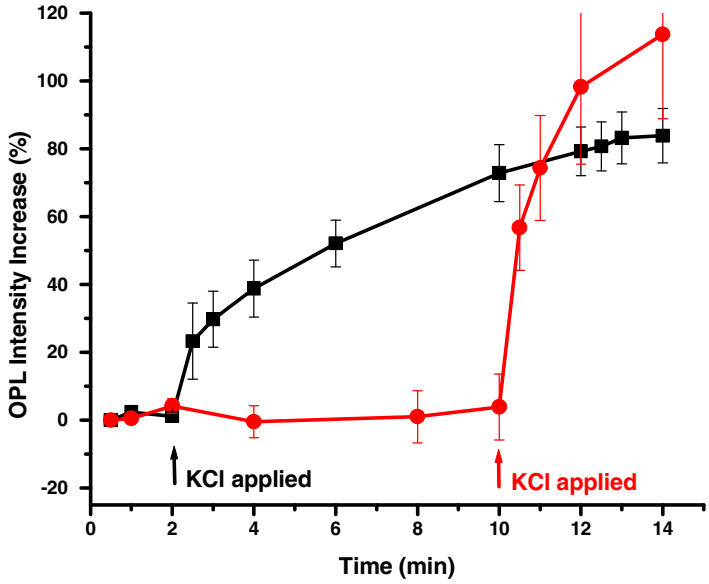

Figure 11. Newport Green intensity increase in the region of the outer plexiform layer (OPL). When 50 mM KCl was applied (left arrow) to retinal slices 2 min after Newport Green application, an immediate intensity increase was observed (squares, ± SEM, n = 5). In controls, when KCl was applied after 10 min (right arrow) in Newport Green, no intensity increase was observed until the time of KCl application (circles, ± SEM, n = 5).

7.4. Zinc Release Discussion

Compared with the extensive literature on the distribution, transport, modulation, and cytotoxic effects of zinc on cortical neurons (Choi et al., 1998), knowledge of the functional role of zinc in the retina is limited. Several studies suggest a role for zinc as a modulator of neuronal responses in both the outer (Kaneda et al., 2002) and inner (Han et al., 1999; Li et al., 2002) retina. Nevertheless, the role of zinc in visual information processing is not well understood (Ugarte et al., 2001).

While several findings summarized above are consistent with a role for zinc as a neuromodulator at the level of the outer plexiform layer as proposed by Wu et al. (1993), direct evidence that zinc is released by depolarization of photoreceptor cells was lacking. The experiments reported here have addressed this issue by observing the fluorescence of the membrane-impermeable form of the Zn^{2+} sensitive dye Newport Green before and after the high potassium-induced depolarization of neurons in the living rat retinal slice. The doubling of fluorescence of the zinc-sensitive dye observed confirms the presence of an increase in extracellular zinc concentration in response to depolarization of retinal neurons (Fig. 9). Since release of synaptic vesicles from photoreceptor terminals has been demonstrated in prior studies using high potassium-induced retinal depolarization (Ripps & Chappell, 1991), we conclude that the band of increased intensity of Newport Green fluorescence observed in the outer plexiform layer (Figs. 9 & 10) demonstrates an increase in vesicular release of Zn^{2+} from rat photoreceptor terminals. This evidence for vesicular release of Zn^{2+} from photoreceptor terminals supports the hypothesis (Wu et al., 1993) that Zn^{2+} is co-released with glutamate from these cells and is available to act as a neuromodulator in the outer retina of vertebrates.

While the finding of depolarization-induced release of Zn^{2+} in the region of the inner segments of rat photoreceptors, on the other hand, seems consistent with evidence for high Zn^{2+} concentration in this region of the light-adapted rat retina reported by Ugarte et al. (1999), we can only speculate concerning the role zinc may be playing in this distal region of the retina. Photoreceptor inner segments are densely packed with mitochondria and photoreceptor mitochondrial respiration has been shown to decrease in light-adapted retina (Perkins, Ellisman, & Fox, 2003). In the region of the inner segments zinc may have a functional significance relative to mitochondrial respiration. Mueller cell apical villi form the outer limiting membrane. It is possible that the Zn^{2+} efflux observed originated from Mueller cell apical villi which surround photoreceptor inner segments.

Mueller cells labeled for zinc transporter protein-3 (ZnT-3) in the region of the apical villi which form the outer limiting membrane in the mouse retina (Redenti et al., 2004). Mueller cells may utilize ZnT-3 to deliver zinc to photoreceptor inner segments during light-adaptation and/or to photoreceptor somata in dark-adapted conditions. Depolarization of Mueller cells by 50 mM K^+ may well result in the release of Zn^{2+} into the extracellular region of the inner segments, especially if the transport involved is electrogenic.

In summary, we conclude from these results that Zn^{2+} is released by depolarization of retinal cells and that this release is highest in the regions of the outer plexiform layer and photoreceptor inner segments. The zinc release observed is likely to include, but is not necessarily limited to, vesicular co-release of Zn^{2+} with glutamate from photoreceptor terminals. In addition, I speculate that Zn^{2+} transport in the region of the Mueller cell apical dendrites and photoreceptor inner segments may be electrogenic and

that Zn^{2+} transport in this region is likely to play a role in photoreceptor mitochondrial function.

Chapter 8

Conclusions and Future Directions

8.1a. Zinc Chelation Electropysiology

The electrophysiological studies presented in this dissertation support a neuromodulatory role for zinc in the outer plexiform layer. As endogenous zinc was chelated in the skate slice preparation, increased inward currents were observed in voltage-clamped horizontal cells. In addition to the increased photoreceptor transmitter release hypothesis, it is possible that the enhanced currents with zinc chelation could reflect the inverse of the known inhibition by zinc of the majority of horizontal cell receptors studied. Results from catfish horizontal NMDA and GABAC, and striped bass AMPA receptors demonstrate consistent current inhibition in the presence of zinc. Half-maximal NMDA, GABAC, and AMPA currents were induced with zinc concentrations between 10-200µM (Wu et al., 1996; Dong et al., 1995; Zhang et al., 2002). Zinc inhibition has been shown to occur on receptor extracellular histidine residues with greatest potency at or near pH. 7.2 (Wu et al., 1996). The effect of histidine as an extracellular chelator then may remove zinc from extracellular fluid and cell surfaces allowing enhanced receptor mediated currents.

As observed in both zebrafish and skate eletroretinogram studies, the removal of endogenous zinc by histidine resulted in enhanced b-wave activity in response to a flash of light. It is known that the ERG is the summed potential of all retinal neurons. In dark-adapted retina, a light flash elicits a negative a-wave from rod cell hyperpolarization, followed by a positive b-wave from bipolar and Mueller cell depolarization (Saszik et al., 2002). The greater b-wave observed in the absence of zinc suggests that transmitter release is increased from photoreceptors and on-center bipolar cells are responding with

depolarizations of increased amplitudes. An appropriate modelof retinal cellular physiology would indicate that zinc inhibits transmitter release and receptor activity thereby increasing ERG thresholds. One relevant experiment demonstrated significantly decreased rat electroretinogram b-wave amplitudes in response to light flashes for at least seven days following intraocular injections of 2 and 4nM zinc sulphate (Nakamichi et al 2003). Bullfrog eyes perfused with 1μM ZnCl exhibited enhancement of ERG thresholds, increased peak amplitudes, and acceleration of rhodopsin regeneration (Kim et al., 2000).

To verify that results seen with histidine are attributable to zinc removal, future studies could utilize other chelators ie. Ca^{2+} EDTA. It is challenging to remove extracellular zinc because eventually zinc diffuses out of cells, possibly becoming bound to membrane surfaces. One approach to silencing the effect of ionic zinc on extracellular receptor sites would be to use iRNA to temporarily inhibit receptor histidine residues. With zinc ion receptor binding sites removed, receptor properties could be evaluated in the absence of zinc effects *in vitro* or *in vivo*. Extended zinc deficiency or chelation studies have been shown to result in a range of dysfunctions from cell signaling inhibition to apoptosis, as discussed previously. To avoid cellular pathogenesis associated with zinc deficiency, iRNA could serve as a transient measure of receptor activity in the absence of zinc modulation. Specific analysis of the role of synaptic zinc can be accomplished by retinal electrophysiology of an existing strain of ZnT-3 knockout mouse (Palmitter et al 1996). If we look at the effect of a lack of vesicular zinc in ZnT-3 knockout mice, we see that only GABA A receptor attenuation was increased in knockouts when compared to wildtypes. (Lopantsev et al., 2003). The implications for retinal physiology in retina

OPL lacking ZnT-3 should be unique considering the graded nature of photoreceptor activity.

Another possible mechanism affected by zinc in retinal tissue is modulation of ephaptic communication within OPL synapses In the invaginations of photoreceptor ribbon synapses, ephaptic communication may be accomplished by currents of horizontal cell dendrites flowing through hemichannels. Such ephaptic communication between horizontal cell and cones is speculated to be involved in negative feedback (Kamermans et al., 2004). A recent study using connexin 35 expressed in oocytes, where voltage was stepped from -20 to +60 in 20mV steps, revealed that 10µM zinc significantly enhanced hemichannel current. In a biphasic manner hemichanel currents were substantially inhibited in the presence of 1mM ZnCl. A simple study to evaluate the role of OPL hemichannels and zinc could measure horizontal cell currents in histidine, carbanoxolone, and 10µM ZnCl, in response to light flashes in intact eyecup preparation.

8.1b. ZnT-3 Immunohistochemistry

The results of analysis of ZnT-3 in retinal tissue revealed positive labeling on Mueller cell soma and processes. This is the first time ZnT-3 has been localized to a glia cell. In all previous studies this transport protein localized to vesicles in terminals containing glutamate or dopamine and zinc (Cole et al., 1999; Danscher et al., 2003; Wenzel et al., 1997; Wange et al 2003.). Mueller transporter localization was verified firstly using immunoperoxidase labeling in the retinal slice and secondly using FITC label in isolated cell culture. Retinal slice preparations showed horizontal bands of ZnT-3

reactivity across the inner segment/outer limiting membrane, outer plexiform/outer nuclear layer, and the ganglion cell layer. These labeled regions were taken to represent regions of Mueller cell membrane concentration. To further clarify cellular localization isolated cell labeling was undertaken revealing Mueller ZnT-3 cell localization. A future study to reveal ZnT-3 localization across intact vertical retinal layers could simply utilize a FITC conjugated ZnT-3 antibody. It is highly probable that Mueller cell fluorescence would reveal ZnT-3 localization from inner to outer limiting membrane. A hypothesis of Mueller cell transport of retinal zinc is plausible considering the role of Mueller cell in transport of a number of important species including K^+, glutamate, and aspartate. (Barbour et al., 1991; Reichenbach et al., 1997).

8.1c. Intracellular Zinc Localization and Extracellular Release

In light-adapted 200µm rat retinal slices intracellular zinc appears most pronounced in outer segments. This study used the zinc probe Zynpyr-1 which exhibits a 4x fluorescence increase upon binding of zinc. Zynpyr-1 is membrane permeable and has the potential to pass into and out of cells. This leaves open the possibility that some zinc fluorescence could involve zinc diffused into the extracellular space. An additional study to specify with greater certainty intracellular zinc levels could use the membrane-trappable zinc probe Zinquin. As Zinquin enters cells and vesicles it binds zinc and becomes trapped to the intracellular space. Accurate measures of zinc localizations in light-adapted tissue could be obtained. It should be noted that the zinc which labels is free or unbound by proteins, leaving an exposed charge which allows probes to bind. Cells

and slices can be imaged using confocal and two-photon microscopy. A next step in determining zinc localization changes would be to visualize zinc in dark-adapted tissue.

Zinc has been shown to be an integral component of the rhodopsin molecule. Increased free intracellular zinc in the outer segments could be available for the higher binding rates to rhodopsin during light-adapted state s (Shuster et al., 1992). Identifying the origin of intracellular free zinc in the outer segments during light adaptation could be accomplished using two-photon microscopic zinc labeling of both isolated and slice intact photoreceptors from dark to light adapted conditions. With real time imaging the protein, organelle, or extracellular source of free zinc could be visualized with minimal light interference.

The origin of extracellular zinc from inner segment regions upon depolarization could be visualized by comparing photoreceptors isolated to those in slice preparations for two-photon analysis. If zinc release is seen only in the slice, then Mueller cell apical villi could be assumed to be releasing zinc into the outer limiting region. Mueller cell endfeet could be releasing zinc into the region of the inner limiting/ganglion cell region. Mueller cells demonstrate the propagation of Ca^{2+} waves from endfeet to soma to apical villi during stimulation with ATP and adenosine (Li et al., 2001). Several calcium imaging dyes have been shown to exhibit an affinity for zinc, therefore Mueller cell measurements for Ca^{2+} signaling may have been showing Zn^{2+} waves through Mueller cells as well (Cheng et al., 1998).

If isolated photoreceptors release outer segment zinc upon depolarization one might look more closely at mitochondria as a source. Mitochondria have been shown to

store and release zinc in response to stimulation (Capasso et al., 2005). Mitochondria take in cytosolic zinc and release it in a Ca^{2+} dependant manner. Submicromolar levels of cytoplasmic zinc decreases mitochondria O_2 consumption and ROS generation, stimulate inner membrane multi-conductance cation channels, and decreases proton motive force (Sensi et al., 2003). Ionic zinc in light-adapted outer segments could be involved in mitochondrial proton force inhibition and conservation of ATP.

Depolarized rat retinal slices released zinc from outer plexiform regions indicating synaptic origin. Slices were light-adapted and hyperpolarized yet still releasing basal levels of transmitter and zinc. Dark-adapted photoreceptors also continuously release transmitter. To prevent transmitter and zinc release through exocytosis of synaptic vesicles, retinal slices can be incubated in Ca^{2+} free solution containing EGTA. To evaluate if release is calcium dependant, slices and or isolated photo receptors can be incubated in solution containing the zinc label Newport Green (extracellular) and allowed to dark-adapt under confocal or two-photon microscopy. Basal transmitter release should be completely inhibited. To induce full tonic release of glutamate and zinc, slices or isolated cells can be exposed to a Ca^{2+} and high K+ and release visualized. To demonstrate Ca^{2+} dependence of zinc release returning EGTA to solution should again fully inhibit synaptic zinc release. A study of Ca^{2+} dependant vesicular release in lizard retinal slice and isolated photoreceptors successfully imaged glutamate vesicular release using two-photon microscopy (Rea et al., 2004), suggesting the feasibility of using this approach.

References

Ahnelt, P. K., H. (1994). Horizontal cells and cone photoreceptors in human retina: a Golgi-electron microscopic study of spectral connectivity. J Comp Neurol *343*.

Akagi, T., Kaneda, M., Ishii, K., and Hashikawa, T. (2001). Differential subcellular localization of zinc in the rat retina. J Histochem Cytochem *49*, 87-96.

Allington, C., Shamovsky, I. L., Ross, G. M., and Riopelle, R. J. (2001). Zinc inhibits p75NTR-mediated apoptosis in chick neural retina. Cell Death Differ *8*, 451-456.
AREDS (2001). A randomized, placebo-controlled, clinical trial of high-dose supplementation with vitamins C and E, beta carotene, and zinc for age-related macular degeneration and vision loss: AREDS report no. 8. Arch Ophthalmol *119*, 1417-1436.

Barbour B, B. H., Attwell D. (1991). Electrogenic uptake of glutamate and aspartate into glial cells isolated from the salamander (Ambystoma) retina. . J Physiol *436*, 169-193.

Behndig, A., Svensson, B., Marklund, S. L., and Karlsson, K. (1998). Superoxide dismutase isoenzymes in the human eye. Invest Ophthalmol Vis Sci *39*, 471-475.

Boycott, B. B. a. W., H. (1991). Morphological classification of bipolar cells of the primate retina Eur J Neurosci *3* 1069-1088.

Bresink, I., Ebert, B., Parsons, C. G., and Mutschler, E. (1996). Zinc changes AMPA receptor properties: results of binding studies and patch clamp recordings. Neuropharmacology *35*, 503-509.

Capasso M, J. J., Malavolta M, Mocchegiani E, Sensi SL. (2005). Zinc dyshomeostasis: a key modulator of neuronal injury. . J Alzheimers Dis *8*, 93-108.

Carmody, R. J., McGowan, A. J., and Cotter, T. G. (1999). Reactive oxygen species as mediators of photoreceptor apoptosis in vitro. Exp Cell Res *248*, 520-530.

Chappell, R., Zakevicius, J., Ripps, H. (2003). Zinc modulation of hemichannel currents in Xenopus oocytes. Biol Bull *205*, 209-211.

Chappell, R. L., Naka, K., and Sakuranaga, M. (1985). Dynamics of turtle horizontal cell response. J Gen Physiol *86*, 423-453.

Chappell, R. L., and Redenti, S. (2001). Endogenous zinc as a neuromodulator in vertebrate retina: evidence from the retinal slice. Biol Bull *201*, 265-267.

Chappell, R. L., and Rosenstein, F. J. (1996). Pharmacology of the skate electroretinogram indicates independent ON and OFF bipolar cell pathways. J Gen Physiol *107*, 535-544.

Chappell, R. L., Zakevicius, J., and Ripps, H. (2003). Zinc modulation of hemichannel currents in Xenopus oocytes. Biol Bull *205*, 209-211.

Cheng C, R. I. (1998). Calcium-sensitive fluorescent dyes can report increases in intracellular free zinc concentration in cultured forebrain neurons. . J Neurochem *71*, 2401-2410.

Choi, D. W., and Koh, J. Y. (1998). Zinc and brain injury. Annu Rev Neurosci *21*, 347-375.

Cole, T. B., Wenzel, H. J., Kafer, K. E., Schwartzkroin, P. A., and Palmiter, R. D. (1999). Elimination of zinc from synaptic vesicles in the intact mouse brain by disruption of the ZnT3 gene. Proc Natl Acad Sci U S A *96*, 1716-1721.

Curcio, C. A., Sloan, K. R., Kalina, R. E., and Hendrickson, A. E. (1990). Human photoreceptor topography. J Comp Neurol *292*, 497-523.

Danscher, G., Wang, Z., Kim, Y. K., Kim, S. J., Sun, Y., and Jo, S. M. (2003). Immunocytochemical localization of zinc transporter 3 in the ependyma of the mouse spinal cord. Neurosci Lett *342*, 81-84.

del Valle, L. J., Ramon, E., Canavate, X., Dias, P., and Garriga, P. (2003). Zinc-induced decrease of the thermal stability and regeneration of rhodopsin. J Biol Chem *278*, 4719-4724.

Dineley, K. E., Votyakova, T. V., and Reynolds, I. J. (2003). Zinc inhibition of cellular energy production: implications for mitochondria and neurodegeneration. J Neurochem *85*, 563-570.

Dong, C. J., and Werblin, F. S. (1995). Zinc downmodulates thf GABAc receptor current in cone horizontal cells acutely isolated from the catfish retina. J Neurophysiol *73*, 916-919.

Dowling, J. E., and Ripps, H. (1977). The proximal negative response and visual adaptation in the skate retina. J Gen Physiol *69*, 57-74.

Faure, P., Benhamou, P. Y., Perard, A., Halimi, S., and Roussel, A. M. (1995). Lipid peroxidation in insulin-dependent diabetic patients with early retina degenerative lesions: effects of an oral zinc supplementation. Eur J Clin Nutr *49*, 282-288.

Feigenspan, A., Gustincich, S., and Raviola, E. (2000). Pharmacology of GABA(A) receptors of retinal dopaminergic neurons. J Neurophysiol *84*, 1697-1707.

Frederickson, C. J., Suh, S. W., Koh, J. Y., Cha, Y. K., Thompson, R. B., LaBuda, C. J., Balaji, R. V., and Cuajungco, M. P. (2002). Depletion of intracellular zinc from neurons by use of an extracellular chelator in vivo and in vitro. J Histochem Cytochem *50*, 1659-1662.

Frederickson, C. J., Suh, S. W., Silva, D., Frederickson, C. J., and Thompson, R. B.

(2000). Importance of zinc in the central nervous system: the zinc-containing neuron. J Nutr *130*, 1471S-1483S.

Gafka, A. C., Vogel, K. S., and Linn, C. L. (1999). Evidence of metabotropic glutamate receptor subtypes found on catfish horizontal and bipolar retinal neurons. Neuroscience *90*, 1403-1414.

Goldstein IM, O. P., Roth S. (1996). Nitric oxide: a review of its role in retinal function and disease. Vision Res *36*, 2979-2994.

Gottesman, J., and Miller, R. F. (1992). Pharmacological properties of N-methyl-D-aspartate receptors on ganglion cells of an amphibian retina. J Neurophysiol *68*, 596-604.

Grahn, B. H., Paterson, P. G., Gottschall-Pass, K. T., and Zhang, Z. (2001). Zinc and the eye. J Am Coll Nutr *20*, 106-118.

Green, D. G., Dowling, J. E., Siegel, I. M., and Ripps, H. (1975). Retinal mechanisms of visual adaptation in the skate. J Gen Physiol *65*, 483-502.

Han, M. H., and Yang, X. L. (1999). Zn2+ differentially modulates kinetics of GABA(C) vs GABA(A) receptors in carp retinal bipolar cells. Neuroreport *10*, 2593-2597.

Han, Y., and Wu, S. M. (1999). Modulation of glycine receptors in retinal ganglion cells by zinc. Proc Natl Acad Sci U S A *96*, 3234-3238.

He, F., Seryshev, A. B., Cowan, C. W., and Wensel, T. G. (2000). Multiple zinc binding sites in retinal rod cGMP phosphodiesterase, PDE6alpha beta. J Biol Chem *275*, 20572-20577.

Hirayama, Y. (1990). Histochemical localization of zinc and copper in rat ocular tissues. Acta Histochem *89*, 107-111.

Hyun, H. J., Sohn, J., Ahn, Y. H., Shin, H. C., Koh, J. Y., and Yoon, Y. H. (2000). Depletion of intracellular zinc induces macromolecule synthesis- and caspase-dependent apoptosis of cultured retinal cells. Brain Res *869*, 39-48.

Kamermans, M., Fahrenfort, I., Schultz, K., Janssen-Bienhold, U., Sjoerdsma, T., and Weiler, R. (2001). Hemichannel-mediated inhibition in the outer retina. Science *292*, 1178-1180.

Kamermans M, F. I. (2004). Ephaptic interactions within a chemical synapse: hemichannel-mediated ephaptic inhibition in the retina. . Curr Opin Neurobiol *14*, 531-541.

Kaneda, M., Andrasfalvy, B., and Kaneko, A. (2000). Modulation by Zn2+ of GABA responses in bipolar cells of the mouse retina. Vis Neurosci *17*, 273-281.

Kaneda, M., Ishii, K., Akagi, T., Tatsukawa, T., and Hashikawa, T. (2005). Endogenous zinc can be a modulator of glycinergic signaling pathway in the rat retina. J Mol Histol *36*, 179-185.

Kaneda, M., Mochizuki, M., Aoki, K., and Kaneko, A. (1997). Modulation of GABAC response by Ca2+ and other divalent cations in horizontal cells of the catfish retina. J Gen Physiol *110*, 741-747.

Kikuchi, M., Kashii, S., Honda, Y., Ujihara, H., Sasa, M., Tamura, Y., and Akaike, A. (1995). Protective action of zinc against glutamate neurotoxicity in cultured retinal neurons. Invest Ophthalmol Vis Sci *36*, 2048-2053.

Kim, H., Kim, Y, Kim, S (2000). Effect of zinc on the visual sensitivity of the bullfrog's eye. . Korean J Ophthalmol *14*, 53-59.

Kokkinou, D., Kasper, H. U., Schwarz, T., Bartz-Schmidt, K. U., and Schraermeyer, U. (2005). Zinc uptake and storage: the role of fundus pigmentation. Graefes Arch Clin Exp Ophthalmol *243*, 1050-1055.

Kolb, H. (1970). Organization of the outer plexiform layer of the primate retina: electron microscopy of Golgi-impregnated cells. Philosophical Transactions of the Royal Society *258*.

Kolb, H., Nelson, R. and Mariani, A. (1981). Amacrine cells, bipolar cells and ganglion cells of the cat retina: A Golgi study. . Vision Res *21*

Koulen, P., Kuhn, R., Wassle, H., and Brandstatter, J. H. (1999). Modulation of the intracellular calcium concentration in photoreceptor terminals by a presynaptic metabotropic glutamate receptor. Proc Natl Acad Sci U S A *96*, 9909-9914.

Kourennyi, D. E., Liu, X., and Barnes, S. (2002). Modulation of rod photoreceptor potassium Kx current by divalent cations. Ann Biomed Eng *30*, 1196-1203.

Land, P. W., and Shamalla-Hannah, L. (2001). Transient expression of synaptic zinc during development of uncrossed retinogeniculate projections. J Comp Neurol *433*, 515-525.

Li, P., and Yang, X. L. (1999). Zn2+ differentially modulates glycine receptors versus GABA receptors in isolated carp retinal third-order neurons. Neurosci Lett *269*, 75-78.

Li, Y., Hough, C. J., Suh, S. W., Sarvey, J. M., and Frederickson, C. J. (2001). Rapid translocation of Zn2+ from presynaptic terminals into postsynaptic hippocampal neurons after physiological stimulation. . Journal of Neurophysiology *86*, 2597–2604.

Li Y, H. L., Russell JT. (2001). Muller cell Ca2+ waves evoked by purinergic receptor agonists in slices of rat retina.

. J Neurophysiol 986-994.

Lin, D. D., Cohen, A. S., and Coulter, D. A. (2001). Zinc-induced augmentation of excitatory synaptic currents and glutamate receptor responses in hippocampal CA3 neurons. J Neurophysiol *85*, 1185-1196.

Lopantsev V, W. H., Cole TB, Palmiter RD, Schwartzkroin PA. (2003). Lack of vesicular zinc in mossy fibers does not affect synaptic excitability of CA3 pyramidal cells in zinc transporter 3 knockout mice. . Neuroscience *116*, 237-248.

Luo, D. G., Li, G. L., & Yang, X. L (2002). Zn2+ modulates light responses of color-opponent bipolar and amacrine cells in the carp
retina. Brain Research Bulletin *58*.

Luo, D. G., and Yang, X. L. (2001). Zn2+ differentially modulates signals from red- and short wavelength-sensitive cones to horizontal cells in carp retina. Brain Res *900*, 95-102.

Malchow, R. P., Qian, H. H., Ripps, H., and Dowling, J. E. (1990). Structural and functional properties of two types of horizontal cell in the skate retina. J Gen Physiol *95*, 177-198.

Malchow, R. P., and Ripps, H. (1990). Effects of gamma-aminobutyric acid on skate retinal horizontal cells: evidence for an electrogenic uptake mechanism. Proc Natl Acad Sci U S A *87*, 8945-8949.

McMahon DG, Z. D., Ponomareva L, Wagner T. (2001). Synaptic mechanisms of network adaptation in horizontal cells. Prog Brain Res *131*, 419-436.

Miceli, M. V., and Newsome, D. A. (1994). Insulin stimulation of retinal outer segment uptake by cultured human retinal pigment epithelial cells determined by a flow cytometric method. Exp Eye Res *59*, 271-280.

Miceli, M. V., Tate, D. J., Jr., Alcock, N. W., and Newsome, D. A. (1999). Zinc deficiency and oxidative stress in the retina of pigmented rats. Invest Ophthalmol Vis Sci *40*, 1238-1244.

Naka, K. I., and Rushton, W. A. (1966). S-potentials from luminosity units in the retina of fish (Cyprinidae). J Physiol *185*, 587-599.

Newsome, D. A., Oliver, P. D., Deupree, D. M., Miceli, M. V., and Diamond, J. G. (1992). Zinc uptake by primate retinal pigment epithelium and choroid. Curr Eye Res *11*, 213-217.

Nicolas, M. G., Fujiki, K., Murayama, K., Suzuki, M. T., Shindo, N., Hotta, Y., Iwata, F., Fujimura, T., Yoshikawa, Y., Cho, F., and Kanai, A. (1996). Studies on the mechanism of early onset macular degeneration in cynomolgus monkeys. II. Suppression of

metallothionein synthesis in the retina in oxidative stress. Exp Eye Res *62*, 399-408.

Okada, T., Fujiyoshi, Y., Silow, M., Navarro, J., Landau, E. M., and Shichida, Y. (2002). Functional role of internal water molecules in rhodopsin revealed by X-ray crystallography. Proc Natl Acad Sci U S A *99*, 5982-5987.

Ou, C. Z., and Ebadi, M. (1992). Pineal and retinal protein kinase C isoenzymes: cooperative activation by calcium and zinc metallothionein. J Pineal Res *12*, 17-26.

Palmiter, R. D., Cole, T. B., Quaife, C. J., and Findley, S. D. (1996). ZnT-3, a putative transporter of zinc into synaptic vesicles. Proc Natl Acad Sci U S A *93*, 14934-14939.

Palmiter, R. D., and Huang, L. (2004). Efflux and compartmentalization of zinc by members of the SLC30 family of solute carriers. Pflugers Arch *447*, 744-751.

Palsgard, E., Ugarte, M., Rajta, I., & Grime, G. W. . (2001). The role of zinc in the dark-adapted retina studied directly using microPIXE. Nuclear Instruments and Methods in Physics Research 489–492.

Perkins, G. A., Ellisman, M. H., & Fox, D. A. (2003). Threedimensional analysis of mouse rod and cone mitochondrial cristae
architecture: Bioenergetic and functional implications. . Molecular Vision *9*, 60–73.

Permyakov, S. E., Cherskaya, A. M., Wasserman, L. A., Khokhlova, T. I., Senin, II, Zargarov, A. A., Zinchenko, D. V., Zernii, E. Y., Lipkin, V. M., Philippov, P. P.*, et al.* (2003). Recoverin is a zinc-binding protein. J Proteome Res *2*, 51-57.

Qian, H., Li, L., Chappell, R. L., and Ripps, H. (1997). GABA receptors of bipolar cells from the skate retina: actions of zinc on GABA-mediated membrane currents. J Neurophysiol *78*, 2402-2412.

Qian, H., Malchow, R. P., Chappell, R. L., and Ripps, H. (1996). Zinc enhances ionic currents induced in skate Muller (glial) cells by the inhibitory neurotransmitter GABA. Proc Biol Sci *263*, 791-796.

Rea R, L. J., Dharia A, Levitan ES, Sterling P, Kramer RH. (2004). Streamlined synaptic vesicle cycle in cone photoreceptor terminals. . Neuron *41*, 755-766.

Redenti, S., and Chappell, R. L. (2002). Zinc chelation enhances the zebrafish retinal ERG b-wave. Biol Bull *203*, 200-202.

Reichenbach, A., Faude, F., Enzmann, V., Bringmann, A., Pannicke, T., Francke, M. (1997). The Mueller (glial) cell in normal and diseased retina: a case for single-cell electrophysiology. Ophthalmic Research *29.*, 326–340.

Ritchie, C. W., Bush, A. I., Mackinnon, A., Macfarlane, S., Mastwyk, M., MacGregor,

L., Kiers, L., Cherny, R., Li, Q. X., Tammer, A.*, et al.* (2003). Metal-protein attenuation with iodochlorhydroxyquin (clioquinol) targeting Abeta amyloid deposition and toxicity in Alzheimer disease: a pilot phase 2 clinical trial. Arch Neurol *60*, 1685-1691.

Rogers, J. M., and Hurley, L. S. (1987). Effects of zinc deficiency on morphogenesis of the fetal rat eye. Development *99*, 231-238.

Rosenstein, F. J., R. W. Miller, and R. L. Chappell. (2001). InvestigOphthalmol Vis Sci *42* S668.

Rosenstein, F. J., and Chappell, R. L. (2003). Endogenous zinc as a retinal neuromodulator: evidence from the skate (Raja erinacea). Neurosci Lett *345*, 81-84.

Saszik SM, R. J., Frishman LJ. (2002). The scotopic threshold response of the dark-adapted electroretinogram of the mouse. J Physiol *543*, 899-916.

Schmidt, K. (1999). Divalent cations modulate glutamate receptors in retinal horizontal cells of the perch (Perca fluviatilis). Neurosci Lett *262*, 109-112.

Sensi, S. L., Canzoniero, L. M., Yu, S. P., Ying, H. S., Koh, J. Y., Kerchner, G. A., and Choi, D. W. (1997). Measurement of intracellular free zinc in living cortical neurons: routes of entry. J Neurosci *17*, 9554-9564.

Sensi, S. L., and Jeng, J. M. (2004). Rethinking the excitotoxic ionic milieu: the emerging role of Zn(2+) in ischemic neuronal injury. Curr Mol Med *4*, 87-111.

Sensi SL, T.-T. D., Sullivan PG, Jonas EA, Gee KR, Kaczmarek LK, Weiss JH. (2003). Modulation of mitochondrial function by endogenous Zn2+ pools. . Proc Natl Acad Sci U S A *100*, 6157-6162.

Shen Y, Y. X. (1999). Zinc modulation of AMPA receptors may be relevant to splice variants in carp retina. Neurosci Lett *259*, 177-180.

Shuster, T. A., Martin, F., and Nagy, A. K. (1996). Zinc causes an apparent increase in rhodopsin phosphorylation. Curr Eye Res *15*, 1019-1024.

Shuster, T. A., Nagy, A. K., Conly, D. C., and Farber, D. B. (1992). Direct zinc binding to purified rhodopsin and disc membranes. Biochem J *282 (Pt 1)*, 123-128.

Shuster, T. A., Nagy, A. K., and Farber, D. B. (1988). 8-Azido-ATP (alpha 32P) binding to rod outer segment proteins. Exp Eye Res *46*, 475-484.

Shuster, T. A., Nagy, A. K., and Farber, D. B. (1988). Nucleotide binding to the rod outer segment rim protein. Exp Eye Res *46*, 647-655.

Smith, J. C., Jr. (1980). The vitamin A-zinc connection: a review. Ann N Y Acad Sci *355*, 62-75.

Spiridon, M., Kamm, D., Billups, B., Mobbs, P., and Attwell, D. (1998). Modulation by zinc of the glutamate transporters in glial cells and cones isolated from the tiger salamander retina. J Physiol *506 (Pt 2)*, 363-376.

Strauss, O. (2005). The retinal pigment epithelium in visual function. Physiol Rev *85*, 845-881.

Stryer, L. (1991). Visual excitation and recovery. J Biol Chem *266*, 10711-10714.

Tabata, T., and Ishida, A. T. (1999). A zinc-dependent Cl- current in neuronal somata. J Neurosci *19*, 5195-5204.

Tate, D. J., Jr., Miceli, M. V., and Newsome, D. A. (1999). Zinc protects against oxidative damage in cultured human retinal pigment epithelial cells. Free Radic Biol Med *26*, 704-713.

Tate, D. J., Miceli, M. V., Newsome, D. A., Alcock, N. W., and Oliver, P. D. (1995). Influence of zinc on selected cellular functions of cultured human retinal pigment epithelium. Curr Eye Res *14*, 897-903.

Tate, D. J., Jr., Newsome, D. A., and Oliver, P. D. (1993). Metallothionein shows an age-related decrease in human macular retinal pigment epithelium. Invest Ophthalmol Vis Sci *34*, 2348-2351.

Tate, D. J., Jr., Newsome, D. A., and Oliver, P. D. (1993). Metallothionein shows an age-related decrease in human macular retinal pigment epithelium. Invest Ophthalmol Vis Sci *34*, 2348-2351.

Ugarte, M., and Osborne, N. N. (1998). The localization of endogenous zinc and the in vitro effect of exogenous zinc on the GABA immunoreactivity and formation of reactive oxygen species in the retina. Gen Pharmacol *30*, 297-303.

Ugarte, M., and Osborne, N. N. (1999). The localization of free zinc varies in rat photoreceptors during light and dark adaptation. Exp Eye Res *69*, 459-461.

Ugarte, M., and Osborne, N. N. (2001). Zinc in the retina. Prog Neurobiol *64*, 219-249.
Vaney, D. I. (1990). The mosaic of amacrine cells in the mammalian retina. Prog Ret Res *9*, 49-100.

Wang, T. L., Hackam, A., Guggino, W. B., and Cutting, G. R. (1995). A single histidine residue is essential for zinc inhibition of GABA rho 1 receptors. J Neurosci *15*, 7684-7691.

Wang, Z. Y., Danscher, G., Dahlstrom, A., and Li, J. Y. (2003). Zinc transporter 3 and zinc ions in the rodent superior cervical ganglion neurons. Neuroscience *120*, 605-616.

Wenzel, H. J., Cole, T. B., Born, D. E., Schwartzkroin, P. A., and Palmiter, R. D. (1997). Ultrastructural localization of zinc transporter-3 (ZnT-3) to synaptic vesicle membranes within mossy fiber boutons in the hippocampus of mouse and monkey. Proc Natl Acad Sci U S A *94*, 12676-12681.

Werblin, F. S. (1991). Synaptic connections, receptive fields, and patterns of activity in the tiger salamander retina. Investigative Ophthalmology and Visual Science *32*, 459-483.

Westerfield, M. (2000). The Zebrafish Book. A Guide for the Laboratory Use of Zebrafish (Danio rerio), 4th ed edn: Univ. of Oregon Press, Eugene).

Wistow, G., Bernstein, S. L., Wyatt, M. K., Behal, A., Touchman, J. W., Bouffard, G., Smith, D., and Peterson, K. (2002). Expressed sequence tag analysis of adult human lens for the NEIBank Project: over 2000 non-redundant transcripts, novel genes and splice variants. Mol Vis *8*, 171-184.

Wu, L., Cao, X. Y., Chen, Y., and Wu, D. Z. (1994). Metabolic disturbance in age-related macular degeneration. Metab Pediatr Syst Ophthalmol *17*, 38-40.

Wu S., M. B. (1998). Amino acid neurotransmitters in the retina: a functional overview. Vision Res *38*, 1371-1384.

Wu, S. M., Qiao, X., Noebels, J. L., and Yang, X. L. (1993). Localization and modulatory actions of zinc in vertebrate retina. Vision Res *33*, 2611-2616.

Wu, X., and Christensen, B. N. (1996). Proton inhibition of the NMDA-gated channel in isolated catfish cone horizontal cells. Vision Res *36*, 1521-1528.

Yang, L., Lu,Shen and Han (2001). Physiological and pharmacological characterization of glutamate and GABA receptors on carp retinal neurons. Progress in Brain Research *131*, 277-293

Yoo, M. H., Lee, J. Y., Lee, S. E., Koh, J. Y., and Yoon, Y. H. (2004). Protection by pyruvate of rat retinal cells against zinc toxicity in vitro, and pressure-induced ischemia in vivo. Invest Ophthalmol Vis Sci *45*, 1523-1530.

Zhang, D. Q., Ribelayga, C., Mangel, S. C., and McMahon, D. G. (2002). Suppression by zinc of AMPA receptor-mediated synaptic transmission in the retina. J Neurophysiol *88*, 1245-1251.